University of Alberta

Signal Dependent Noise and its Role in Motor Planning

by

Yi Mao

©

A thesis submitted to the Faculty of Graduate Studies and Research
in partial fulfillment of the requirements for the degree of

Master of Science

Department of Biomedical Engineering

Edmonton, Alberta
Fall 2006

Library and Archives Canada

Published Heritage Branch

395 Wellington Street
Ottawa ON K1A 0N4
Canada

Bibliothèque et Archives Canada

Direction du Patrimoine de l'édition

395, rue Wellington
Ottawa ON K1A 0N4
Canada

Your file Votre référence
ISBN: 978-0-494-22317-8
Our file Notre référence
ISBN: 978-0-494-22317-8

NOTICE:
The author has granted a non-exclusive license allowing Library and Archives Canada to reproduce, publish, archive, preserve, conserve, communicate to the public by telecommunication or on the Internet, loan, distribute and sell theses worldwide, for commercial or non-commercial purposes, in microform, paper, electronic and/or any other formats.

The author retains copyright ownership and moral rights in this thesis. Neither the thesis nor substantial extracts from it may be printed or otherwise reproduced without the author's permission.

AVIS:
L'auteur a accordé une licence non exclusive permettant à la Bibliothèque et Archives Canada de reproduire, publier, archiver, sauvegarder, conserver, transmettre au public par télécommunication ou par l'Internet, prêter, distribuer et vendre des thèses partout dans le monde, à des fins commerciales ou autres, sur support microforme, papier, électronique et/ou autres formats.

L'auteur conserve la propriété du droit d'auteur et des droits moraux qui protège cette thèse. Ni la thèse ni des extraits substantiels de celle-ci ne doivent être imprimés ou autrement reproduits sans son autorisation.

In compliance with the Canadian Privacy Act some supporting forms may have been removed from this thesis.

While these forms may be included in the document page count, their removal does not represent any loss of content from the thesis.

Conformément à la loi canadienne sur la protection de la vie privée, quelques formulaires secondaires ont été enlevés de cette thèse.

Bien que ces formulaires aient inclus dans la pagination, il n'y aura aucun contenu manquant.

Canada

Abstract

The recently proposed minimum variance theory showed promise in explaining underlying strategy of motor planning. It assumed the presence of a linearly-scaling signal dependent noise (SDN) corrupting the motor command and suggested that the goal of motor planning is to minimize movement variability caused by SDN. To investigate the validity of this assumption, force SDN was measured as an approximation for the motor command SDN. The scaling of this noise was non-linear. Furthermore, the SDN generated from static and dynamic contractions were shown to be different, but the difference was only significant at low forces. To investigate the effect of non-linear noise on the minimum variance theory, simulations were performed under linear and non-linear noise conditions using a redundant wrist model. Results showed that the non-linear noise did not significantly increase variability of wrist movements and likely would not alter the predictions of the minimum variance theory significantly.

Acknowledgements

I would like to express my profound gratitude to my supervisor Dr. Kelvin E. Jones for his support and guidance with this thesis. I am indebted to the other members of my thesis committee, Dr. Richard Stein and Dr. David Collins for insightful feedback in helping to improve the quality of my work. I must also thank my parents and my friends who provided me with the support and inspiration that I needed to get through my degree.

Table of Contents

Table of Contents 3

List of Tables 7

List of Figures 8

List of Figures 8

1 Introduction 1

1.1 Importance of Movement 1

1.2 Approaches to the Study Movement 3

1.3 Layout of Thesis 4

2 Background and Motivation 6

2.1 Making Movements 6

2.1.1 The Descending Motor Pathways 6

2.1.2 The Muscle and the Motor Unit 7

2.2 Invariant Features of Movement 13

2.3 Movement Planning Strategies 14

2.4 The Minimum Variance Theory 15

2.4.1 Predicting Kinematics 18

2.4.2 Predicting Muscle Activation Patterns 21

2.5 Signal Dependent Noise 24

2.5.1 Defining SDN 24

2.5.2 Relevance of SDN 26

2.5.3 Origin of SDN 27

2.5.4 Characterizing SDN 31

2.6 Project Goals 34

3 Methods 37

3.1 Data Collection 37

3.1.1 Subject Recruitment 37

3.1.2 Experimental Setup 37

3.1.3 Data Acquisition 38

3.1.4 Experimental Protocol 38

3.1.5 Training 40

3.2 Data Analysis 41

3.2.1 Pre-Processing 41

3.2.2 Hypotheses Testing 43

4 Results 52

4.1 SDN Under Different Types of Contractions 53

4.2 Scaling of SDN 55

4.3 Effect of Non-linear SDN 58

5 Discussion 62

5.1 Different Contraction Types Produce Different SDN 62

5.2 The SDN Scales Non-linearly With Mean Force 64

5.3 Effect of Non-linear SDN 68

5.4 Limitations of the Wrist Model 68

6 Conclusions & Future Work 70

7 References 72

List of Tables

Table 4.1: CV curve fitting parameters..... 56

List of Figures

Fig 2.1: Descending motor pathways 7

Fig 2.2: The motor unit and the motor neuron pool 8

Fig 2.3: Types of motor units 10

Fig 2.4: Fusing of twitch forces. 11

Fig 2.5: Orderly recruitment. 12

Fig 2.6: Minimizing end position variance in a directed movement 16

Fig 2.7: Simulated vs expermental trajectories 19

Fig 2.8: Minimum Variance predicts the 2/3 power law 19

Fig 2.10: Muscle activation patterns during wrist movements 23

Fig 2.11: Idealized SDN. 24

Fig 2.13: Motor unit pool simulations with different recruitment orders 29

Fig 2.14: Voluntary and NMES induced contractions. 30

Fig 2.15: Force CV and SD (Moritz et al, 2004). 33

Fig 2.16: Force SD vs Mean Force (Slifkin &Newell, 1999) 34

Fig 3.1: Experimental protocols for the thee types of contraction 39

Fig 3.2: Screen shot of spike2 during training 40

Fig 3.3: Processing of raw data 42

Fig 3.4: Force binning 43

Fig 4.1: Raw force traces 52

Fig 4.2: CV and SD vs mean force 53

Fig 4.3: CV vs mean force 55

Fig 4.4: CV and SD vs mean force 57

Fig 4.5: Simulated trajectories 59

Fig 4.6: Simulated end position coordinate errors 60

Fig 4.7: Comparison of the error ellipse areas under different noise conditions. 61

Fig 5.1: Contraction speed and recruitment order. 63

Fig 5.2: Comparison of CV and SD data from four studies 66

1 Introduction

1.1 Importance of Movement

The most obvious characteristic that distinguishes a living organism from one that is dead is movement, and in most cases, movement is an essential function that enables the living organism to stay alive. Animals in the wild must move to search for food and escape from predators, and even though advanced technologies and cooperative societies have sheltered us from such primitive activities, most of us must still, on occasion, walk to the store to purchase groceries, or drive away on a vacation to escape the tedium of everyday life.

A body movement, as simple as pointing a finger, requires a complex cascade of neural commands initiated from the brain to activate a set of muscles in a highly coordinated manner. Even though such complex control and coordination is required to execute a movement, we often make such movements without even a conscious thought. As described by American psychologist Robert S. Woodworth: 'When I voluntarily start to walk, my intention is not of alternately moving my legs in a certain manner; my will is directed toward reaching a certain place. I am unable to describe. … what movements my arms or legs are going to make; but I am able to state what result I design to accomplish' (1906, p. 375). Thus, at a cognitive level, the act of walking is represented as a simple goal-directed displacement of the body, while at the execution level, neural commands

and muscle activation patterns constitute the components of movement that the subject is oblivious to (Jeannerod, 1988). However, the detailed mechanisms of the neural process that links the cognitive intent of displacing oneself to the execution details of activating the necessary leg muscles remains a well guarded secret of the nervous system. Yet, when something goes awry in these processes, the effects are often highly visible and severely detrimental to the subjects.

The nature of movement disorders can vary immensely: from hyperkinetic disorders (excess of movement), to hypokinetic disorders (scarcity of movement), and the extreme case of akinesis (absence of movement). The negative effects of movement disorder can range from mild embarrassment from slightly uncoordinated movements to the inability to feed oneself or perform other activities of daily living. The various disorders typically result from damage or abnormalities at sites in the nervous system involved with controlling movement. The possible causes of such damage or abnormalities are seemingly endless: various forms of neurodegenerative diseases such as Parkinson's and Huntington's, physical trauma to the nervous system, stroke, and chemical toxins to name a few. Consequently the number of people afflicted with movement disorders is quite extensive. Furthermore, because of our inadequate understanding of the nervous system, our means of inducing complete recovery in patients afflicted with motor disorders are very limited. Thus, acquiring a clear understanding of movement is a daunting, but potentially very beneficial pursuit.

1.2 Approaches to the Study Movement

Many different approaches to the study of movement have been employed in the past. Psychophysical experimentation involving target movements of various types toward visual stimuli is one of the more traditional approaches to the study of movement and has its roots in the field of psychology. Studying motor impairment in animals with lesions at various points in the nervous system, as well as in humans with certain neurological diseases, has also yielded a great deal of information regarding the various neural structures involved in motor control. Furthermore, as movements are the direct result of pulling forces generated from specific patterns of muscle contractions, studying the force output of various types of contractions in different muscles can also be very educational.

With the tremendous advancements in the capabilities of computer technologies made in recent decades, computer modeling has become a very useful tool in the field of motor control, as well as many other fields of scientific research.

Computer modelling can be approached in two different ways: using a top-down approach, or a bottom-up approach. The bottom-up approach implements a model that focuses on low level components and mechanisms of the system that have been observed empirically. By striving to include all the essential low level details of the system, the model may be able to emulate the high level behaviour of the system. Contrastingly, the top-down approach typically starts with the assumption of some unifying principle that provides a general framework which guides the behaviour of the system. By implementing a simplistic model that only includes the high level functional components

of the system, with their interactions and overall behaviour guided by the assumed principle, the model is able to support the validity of the unifying principle if it can produce accurate predictions of the system output. Thus, regardless of the approach taken, the validity of any model lies in its ability to accurately predict the output of the system that it is attempting to mimic in real life situations.

In this thesis, force data obtained experimentally from human muscle contractions is used to modify a computer model of a potential optimization strategy used by the nervous system to select an appropriate trajectory for a specific movement. Thus, we are employing both experimental and modeling techniques to achieve the set of research goals that we have proposed. The model of interest is of the top-down variety, and it may reveal a great deal about how trajectory planning is achieved in the nervous system.

1.3 Layout of Thesis

The thesis is organized into a number of chapters. The first chapter, Background and Motivations, provides the necessary background information that may assist a reader who is not an expert in the field in understanding the theory behind the work done in this thesis. The topics discussed are: neurological mechanisms in the execution of muscle contractions and bodily movements, potential control strategies to produce accurate movements, proposed minimum variance theory of motor planning and the relevance of signal dependent noise to this theory. Furthermore, the chapter also presents a summary of the relevant research pertaining to the minimum variance theory and noise in the neuromuscular system, which provides the antecedent for the work done here. Lastly, the

Background chapter defines the goals of the thesis project in the form of specific questions that are to be addressed. Essentially, this chapter will explain why we are interested in signal dependent noise and what specific issues we intend to address with regards to the noise. The Methods chapter provides a detailed description of the protocol used to collect the experimental data as well as the analysis performed to extract the relevant information that will enable us to answer the questions outlined in the Background and Motivation chapter. The Results chapter presents the outcomes obtained from the analysis of the data collected such that conclusions may be drawn pertaining to the research questions of interest. The Discussion and Conclusion chapter interprets the results presented in the previous section by examining what they reveal about signal dependent noise and the implications with respect to the minimum variance theory.

2 Background and Motivation

2.1 Making Movements

Voluntary movement of the body is an essential part of everyday life. We move our legs to walk to from one location to another. We move our arms when we want to reach for a certain object. We move our heads when we want to look in a particular direction. The physiological process behind the control of the musculoskeletal system in making movements is highly complex, yet we are able to initiate and execute the movements with only a simple thought. This section will provide an overview of the physiological processes involved in achieving a coordinated movement.

2.1.1 The Descending Motor Pathways

Movement is achieved through the coordinated contractions of a set of appropriate muscles, which causes rotation at the appropriate joints leading to displacement of the designated body part. The planning and executions of these contractions are under the control of the Central Nervous System (CNS), which relays its commands to the muscles via the descending motor pathways (Fig. 2.1). The initiation and preliminary planning of a voluntary movement begins in the CNS at the premotor areas, which includes the premotor cortex and the supplementary motor area. Necessary visual information, such as location of a target object, is provided through the posterior parietal cortex. Supplemented with the relevant visual information, the motor cortex then produces a

detailed motor program that determines the activation sequence of the appropriate muscle groups. This motor program is then relayed, via upper motor neurons, to the spinal cord, and eventually to the lower motor neurons that directly innervate the necessary muscles. The lower motor neurons then excite the muscle to the level specified by the motor command, and the excited muscle contracts to generate pulling forces at the connected joints, thereby producing the final output of the motor system.

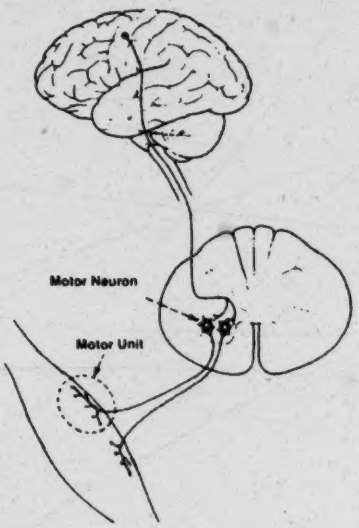

Fig 2.1: Descending motor pathways (Original Think Tank 2006)

2.1.2 The Muscle and the Motor Unit

To produce a simple movement of the body, the appropriate muscles must contract to generate the necessary torques about the corresponding joints, such as the shoulder, elbow and wrist for an arm movement. The amount of contractile force generated by the muscles dictates the torque applied to each joint, which in turn determines the acceleration of the body segment involved in the movement. In such a way, the

contractile forces produced by the muscles that control the joints can influence the trajectory and speed of various movements of the body.

A muscle in the human body can be comprised of thousands of motor units, with each motor unit consisting of a single motor neuron and the muscle fibers that it innervates (Fig 2.2). The number of fibers innervated by a single motor neuron ranges from just a few, as in the case of the human extra-ocular muscles (Feinstein *et al*, 1955), to as many as a few hundred, as in the biceps brachii (Christensen *et al*, 1959). Within a muscle, the fibers of each motor unit are interleaved with fibers of neighbouring motor units such that they are generally distributed throughout a somewhat localized area in the cross section of the muscle.

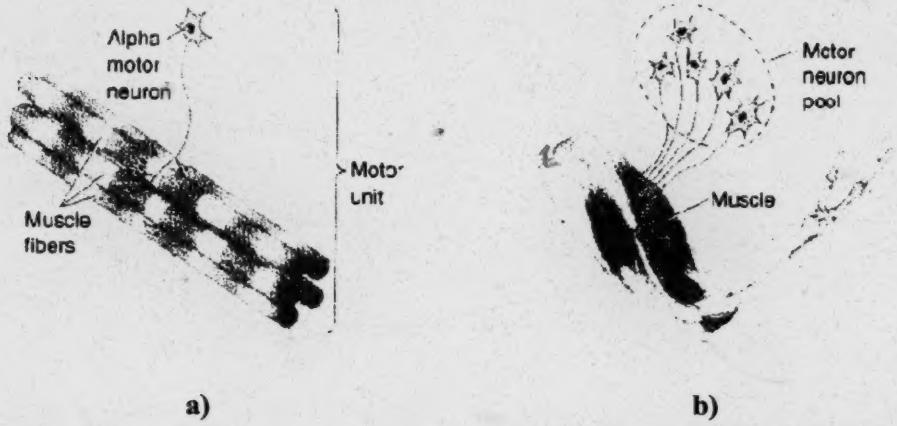

Fig 2.2: The motor unit and the motor neuron pool. a) The motor unit and its constituent motor neuron and muscle fibers, b) Motor neurons of motor unit pools receive a common descending drive. (Martini 2004)

Motor units are the simplest contractile elements within the muscle. They are typically differentiated into one of three groups, according to their twitch forces and their fatigability (Fig 2.3). The twitch force of a motor unit is the force profile generated from

the synchronous contraction of all the innervated fibers, and fatigability is a measure of the rate at which the peak force produced by a fiber decreases over repeated contractions. The motor units that produce the smallest twitch forces with very slow rise and fall times and are capable of maintaining their initial level of twitch force over a long period of repeated contractions are called slow (S) units. These units consist of slow oxidative (SO) fiber. On the other hand, motor units that produce the largest twitch forces, typically with very fast rise and fall times, consists of fast glycolytic (FG) fibers. They tend to show marked decreases in the magnitude of their twitch force after a short period of repeated contractions. These units are referred to as fast fatigable (FF) units. The third class of motor units, comprised of fast oxidative glycolytic (FOG) fibers are intermediate in terms of twitch force profile and fatigability, compared to the other two types of motor units and are called fast fatigue resistant (FFR) units. The muscle fibers within a particular motor unit are all of the same type. These fibers respond together, in an all-or-none fashion, to excitation from the innervating motor neuron. As action potentials of the motor neuron travel down the axons, neurotransmitter is released into the neuromuscular junctions, causing depolarizations (end plate potentials) on the surface membrane of the fibers. If threshold is reached, then muscle action potentials are triggered on the fiber membranes, which trigger the release of intracellular Ca^{+} stores and thereby induce contraction of the fibers. The resulting motor unit twitch force produced is the sum of the twitches from all the constituent fibers within the motor unit. As such, the profile of the twitch force is unique to a particular motor unit, since it is a function of the quantity and characteristics of the constituent fibers.

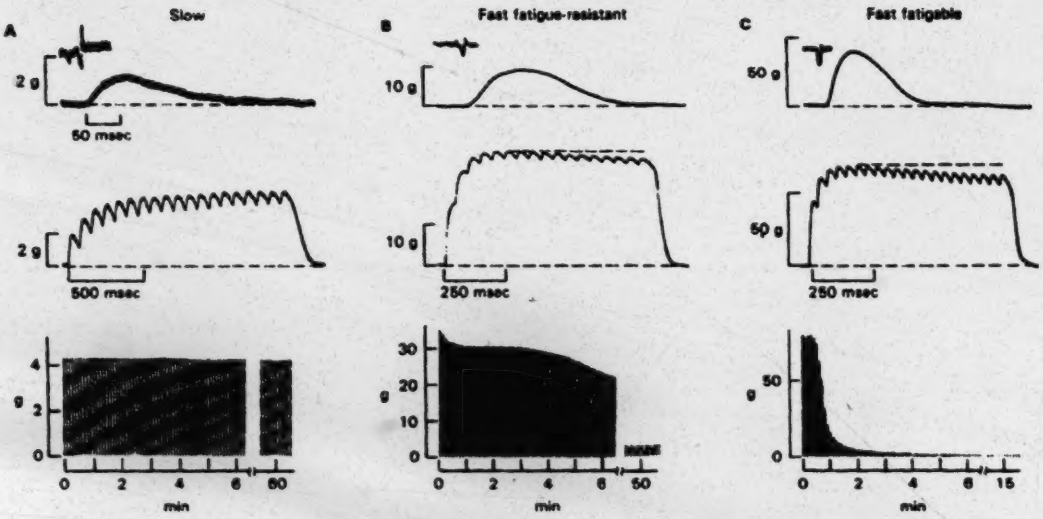

Fig 2.3: Types of motor units. a) Twitch forces of Fast Glycolytic (FG), Fast Oxidative Glycolytic (FOG) and Slow Oxidative fibers. b) Fatigue curves showing the change in force as a function of contraction time for the three types of fibers (Burke and Tsairis, 1974).

For each motor unit action potential, a motor unit twitch force is generated. Since a twitch force is longer in duration than an action potential, when repetitive firing of the motor neuron exceeds a certain rate, the twitch forces resulting from successive action potentials fuse together and demonstrate a summing effect. In this manner, as the discharge rate of motor unit action potentials increase, the mean force produced by the motor unit will also increase until the twitch forces are completely fused together, producing a relatively smooth and continuous force output, a condition called tetanus (Fig 2.4). Thus, when the motor neuron is firing at a relatively low rate, the force produced by the motor unit is highly variable. Only at higher levels of activation can a consistent level of force be generated. Furthermore, as slow units have longer twitch forces, fusion of the twitches begins at lower motor unit firing rates.

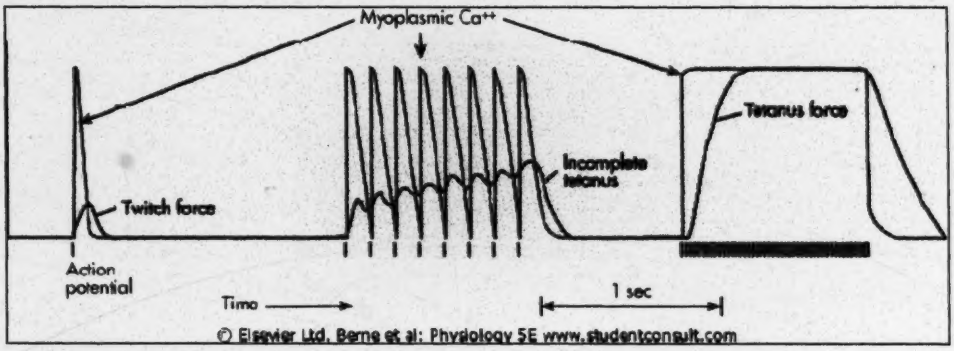

Fig 2.4: Fusing of twitch forces. As firing rate increases, successive twitches gets closer together and eventually fuses into a smooth titanic force. (Berne 2003)

Within most skeletal muscles, motor units of all three fiber types can be found. Though the relative proportion of the different types of fibers can vary depending on the nature of the muscle, there are typically a greater number of slow twitch units compared to the larger fast twitch units. Consequently, as the excitatory drive to the muscle is gradually increased, the step size of the increase in force output that results from the activation of each additional unit also increases.

As each muscle consists of a large number of motor units, the force output of a muscle can be influenced by the number of motor units active, as well as the level of activation (firing rate) in each of the motor units. A motor unit is activated when the synaptic drive from higher centers in the CNS exceeds the threshold of the motor neuron, thereby causing the neuron to spike. This motor unit recruitment threshold typically shows some variability, and thus, is more of a probability function rather than a discrete cutoff. Essentially, as the synaptic drive increases, the likelihood of a particular motor unit being recruited increases as well.

The recruitment of motor units within a muscle follows a particular order that is fairly consistent across a number of different types of activities. The idea is that all the motor units within a motor unit pool have different activation thresholds. As such, the units with lower thresholds tend to be recruited before the units with higher thresholds. In general, the units producing the smallest twitch forces with the slowest contraction times are typically recruited first. Progressively, units with larger force and faster contraction times are recruited. In effect, S units are typically recruited first, followed by the FFR units, and finally the FF units (Fig 2.5). Thus, a motor unit twitch force seems to provide a good indicator of recruitment order (Milner-Brown, Stein et al. 1973; Dengler, Stein et al. 1988).

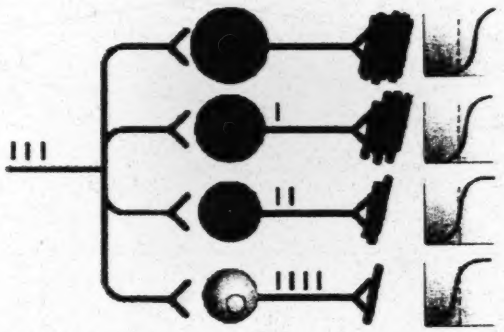

Fig 2.5: Orderly recruitment. Units with smaller twitch forces, illustrated by smaller number of fibers, tend to be recruited earlier at lower excitatory inputs (Stein et al 2005).

The nervous system achieves an increase in force output of a muscle by increasing the descending motor drive, which will gradually recruit more motor units within the muscle. The motor units being recruited will have increasingly larger twitch amplitudes, so the force increase resulting from motor unit recruitment will occur in bigger and bigger steps. Furthermore, the increasing motor drive will cause increase in the firing rate of the motor

units that have already been recruited, which will increase the force output of these activated units until they reach their limit.

2.2 Invariant Features of Movement

There is a great deal of flexibility and redundancy in the musculoskeletal structure of humans. As such, there are countless possible trajectories to choose from when executing a movement. To complicate things further, any particular trajectory can be achieved through a number of different muscle activation patterns.

Despite the countless ways that a single movement can be generated, there tends to be some degree of stereotypy in human movements. Certain invariant features are observed in a variety of movements and are reproducible across subjects and over many trials.

For any particular goal directed movement of the arms, the trajectory taken tends to be similar over numerous trials. These trajectories are typically fairly straight and very smooth (Flash and Hogan 1985). Furthermore, the velocity profiles generated from these smooth trajectories tend to be symmetrical about the mid point of the movement duration and approximate a bell shaped curve. Similar velocity profiles are also observed during saccades, though the profiles tend to become asymmetrical during large amplitude eye movements.

For arm movements in humans, there appears to be an inherent trade off between the speed with which the movement is performed and the accuracy of the arm in reaching a

designated target. In fact, the relationship has been captured mathematically by an equation known as Fitts' Law (Fitts 1954).

Another law that captures a stereotyped feature of arm movement is the 2/3 power law ; Viviani & Schneider, 1991). This law describes the relationship between hand velocity and radius of curvature during curved arm movements: the greater the curvature, the slower the hand moves. These two variables are related according the equation: $V = KR^{(1-\beta)}$, where V and R are the velocity and radius, respectively, while the exponent β is approximately equal to 2/3.

2.3 Movement Planning Strategies

Considering that there are potentially an infinite number of paths that can be taken during a simple goal directed movement and yet the same path is always chosen, it seems logical that the motor control system is performing some form of optimization that allows it to arrive at the same optimal trajectory every time. Several optimization strategies have been proposed in the past, each of which captures a certain stereotypical feature of natural movement.

One logical choice for an optimization scheme would be to minimize the energy expenditure required to execute a movement, as such a strategy would seem beneficial in an evolutionary sense. However, during fast movements, trajectory overshoot is typically observed. An energy minimization strategy cannot predict an overshoot, as overshoots

and the necessary corrective movement would require consumption of excess energy, in comparison to a direct path movement.

Observing that goal directed movements tend to be smooth, Flash and Hogan (Flash and Hogan 1985) proposed that an optimal trajectory is selected by making the movement as smooth as possible, or equivalently, minimizing the jerk. Jerk is the derivative of acceleration, and is thus inversely proportional to smoothness. On a similar note, Uno et al (1989) proposed that optimal trajectory may be selected based on a minimum torque change criterion. As torque is related to angular acceleration, this is analogous to angular jerk at the joints. Although these models are able to reproduce a limited range of empirical data, it is unclear why smoothness is important during movements, or how complex quantities such as jerk or torque change could be measured in the nervous system. The models are simply designed to generate output that mimics experimental observations, and thus do not provide any insight to the mechanisms that are responsible for the observed behaviours.

2.4 The Minimum Variance Theory

An alternative proposal for a motor planning strategy is to minimize the end point variance of goal directed movements caused by noise inherent in the motor system . The premise for this theory is the assumption that there is a biological noise present in the neuromuscular system. This noise increases in magnitude as the mean level of motor command increases and is thus termed Signal Dependent Noise (SDN). It will be described in more detail in the following section. During the execution of a movement,

this noise corrupts the motor command, thereby causing the movement trajectory to deviate from the desired path. The disruptive effect of the noise accumulates over the duration of the movement, resulting in an error in the terminal position from the desired target of the movement. Moreover, due to the noise, the same sequence of intended motor commands repeated over many trials, will not produce the same movement every time, but will rather result in a probability distribution of terminal positions (Fig 2.5), which may be quantified by its variance.

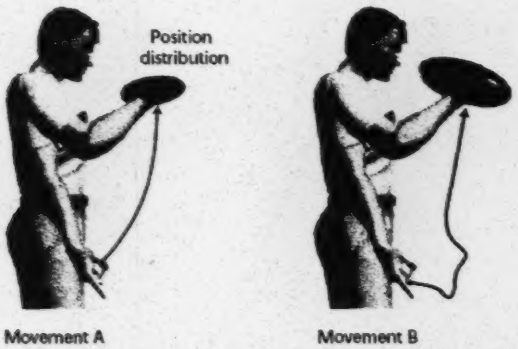

Fig 2.6: Minimizing end position variance in a directed movement. Following an optimal trajectory (Movement A), which happens to be relatively smooth, results in a smaller end point error distribution, while the non optimal trajectory (Movement B) generates a larger spatial distribution of end point errors. (Wolpert and Ghahramani 2000)

As the noise is stronger at higher levels of motor command, its disruptive effects are more significant for quicker movements, which require more forceful contractions. Thus, the minimum variance approach must strike a balance between terminal precision of the movement and the relative speed of the movement. Given a fixed time constraint for the execution of the movement, the cost function to be minimized in applying the minimum variance strategy is the error (or variance) in the terminal position of the movement. Alternatively, the minimum variance strategy can also be described as the minimization

of the movement duration when an end point variance constraint, appropriate for the task at hand, is specified prior to the commencement of the movement.

This strategy is attractive because it is behaviourally relevant, as the target quantity of the optimization is directly correlated to the successful completion of a goal-directed movement task. The greater the terminal variance of a movement, the greater the deviation from the desired target a single instance of the movement is likely to be, and thus, the greater the probability of failure in achieving the specified goal. Therefore, minimizing the end point variance directly contributes to the completion of the desired movement.

Although the quantity to be optimized results from the disruptive effects of the noise accumulated over the duration of the movement, it can be easily measured from readily available cues at the end of the movements. There would be no need to integrate complex quantities over the movement period, as was the case for the aforementioned control strategies.

Some obvious and apparent cues that could serve the purpose of the error signal include distance between actual limb position and the desired target position, or time required to execute corrective movements to reach the intended target. In fact, climbing fibers in the cerebellum have been shown to code for a positional error signal at the end of movements (Kitazawa 2002). The measured error signal can then be used to train the nervous system

to improve the execution of similar movements in the future, thereby contributing to motor learning with repetitions of the movement.

2.4.1 Predicting Kinematics

In the Harris and Wolpert study (1998), simulations of planar arm movements were performed using a two-joint nonlinear arm model consisting of two linear second order muscles pulling at the shoulder joint and the elbow joint. To generate the trajectory of a point to point movement, a signal dependent noise corrupting the motor command was introduced to the system and the minimum variance strategy was applied. By optimizing for the positional variance in the presence of the noise, the model was able to predict the various stereotyped features of human arm movements, as well as saccadic eye movements.

The smooth and relatively straight hand paths predicted by the model for point to point movements are shown in figure 2.7 alongside actual trajectories of movements obtained experimentally, with similar start and end points. Note that the smoothness of the movement trajectory is now a secondary result of optimizing for a task relevant cost rather than being the direct goal in movement planning. The symmetric bell shaped velocity profiles of the arm movements are also predicted by the model, as shown in the same figure.

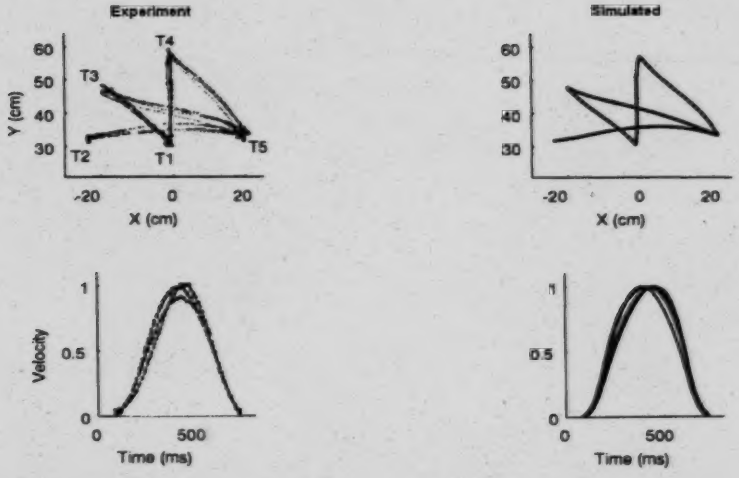

Fig 2.7: Simulated vs expermental trajectories. Simulated (right side) and actual (left side) hand paths and velocity profiles of planar arm movements (Harris and Wolpert 1998).

Figure 2.8 shows simulation results of arm movement in an elliptical path. The optimal trajectory chosen under minimum variance control reproduces the empirical two-thirds power law. The graph on the left shows spatial location at equidistant points in time, while the graph on the right shows the log-log relationship between curvature radius (R) and movement velocity (V). The slope of the relationship is 1/3, which results in a β of 2/3 in the equation: $V = KR^{(1-\beta)}$, as required by the two-thirds power law .

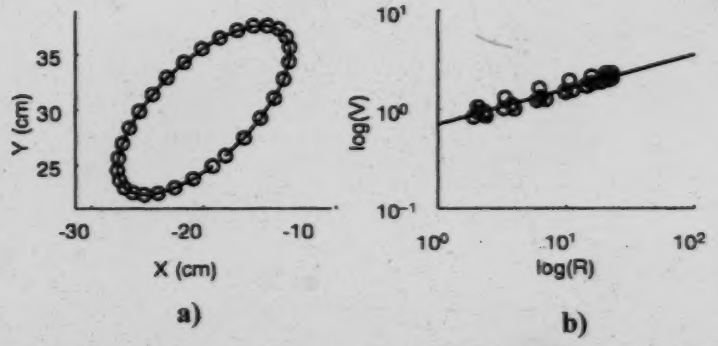

Fig 2.8: Minimum Variance predicts the 2/3 power law. a) simulations of elliptical hand movement, all adjacent points are equidistant in time, the closeness of the points at the apices indicate a decrease in velocity. b) plot of velocity against radius of curvature in log scale shows slope of 1/3, which gives β of 2/3 (Harris and Wolpert 1998).

Furthermore, it was demonstrated that the speed accuracy trade off is also a natural outcome of trajectory planning using the minimum variance strategy, since faster movement requires larger motor commands, which are accompanied by higher noise levels, thus resulting in increased variability in movement. In fact, the exact mathematical relationship described by Fitts' was reproduced using a one dimensional arm model.

Lastly, velocity profiles of saccadic eye movements, generated from a linear third order model of the eye (Robinson, Gordon et al. 1986), employing the minimum variance strategy in the same manner as the arm model, are shown below in figure 2.9 alongside experimentally obtained velocity profiles. In both cases, the profiles are bell shaped and symmetric for small amplitude saccades, but become increasingly non symmetrical as the amplitude increases above 30°.

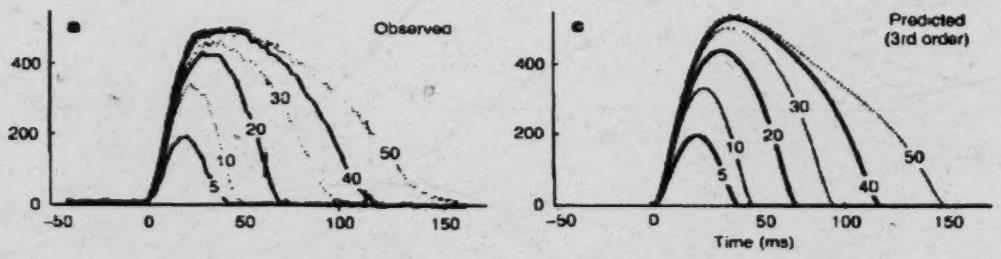

Fig 2.9: Velocity profiles for simulated and experimental saccades. Velocity profiles of saccades for different amplitudes (in degrees), a) is observed experimental data and b) is the predicted velocity profile from a third order model using the minimum variance control strategy (Harris and Wolpert, 1998).

2.4.2 Predicting Muscle Activation Patterns

Using a wrist model, Haruno et al (2005) were able to show that, in addition to predicting the distinct features in the kinematics of human arm and eye movements, the minimum variance theory is also able to predict the characteristic muscle activation patterns during wrist movements. The wrist model is comprised of five muscles, each with a unique pulling direction, as is the case in the primate wrist. The muscles are modeled as identical second order linear systems (Van der Helm and Rozendaal 2000) that convert input motor commands to force outputs, same as those used in the Harris and Wolerert study (1998). By summing the pulling forces of each muscle in their respective direction, a positional change of the wrist can be determined from the temporal sequence of motor commands to the five muscles.

The organization of the muscular and skeletal system creates a level of redundancy in the control of the wrist, which is reproduced in the model, as there are 5 muscles pulling in an effectively 2 dimensional plane. Despite this redundancy, which allows any particular trajectory to be generated in a number of different motor command sequences, the muscle activation pattern of human wrist movements is nonetheless highly stereotyped . It has been shown that for any particular wrist movement, each wrist muscle may act as either an agonist (pulling in the direction of movement) or an antagonist (pulling against the direction of movement). The muscles behaving as agonists always show two agonist EMG bursts, a large one followed by a smaller one, while the antagonist muscles show only one antagonist EMG burst, which occurs between the two bursts of agonist muscles. As long as the behaviour of the muscle remains the same (i.e. acting as agonist or

antagonist), the timing of the bursts remains stationary and only the burst amplitude is modulated with changes in direction.

Applying the minimum variance control strategy, the model assumes the presence of an SDN, and computes the optimal sequence of motor commands required to move the wrist to the required target with minimal end positional variance. Surprisingly, the resulting optimal motor commands produce a spatiotemporal activation pattern in the wrist muscles that greatly resembles the pattern seen in empirical data. Figure 2.10 b) shows the muscle activation patterns predicted by the model, each colour representing a movement toward a target in a different direction. Note the presence of either two agonist bursts near the beginning and end of the movement, or a single antagonist burst in the middle of the movement for any single muscle during any particular movement. The timing of the bursts remains the same within each muscle and only the amplitude is modulated. Figure 2.10 c) shows, with more detail, a side by side comparison of simulated data and experimental data for extensor. carpi radialis longus (ECRL) and extensor carpi ulnaris (ECU). The relative timing and amplitude of the peaks within each muscle for movements in the various directions are very similar in the two data sets.

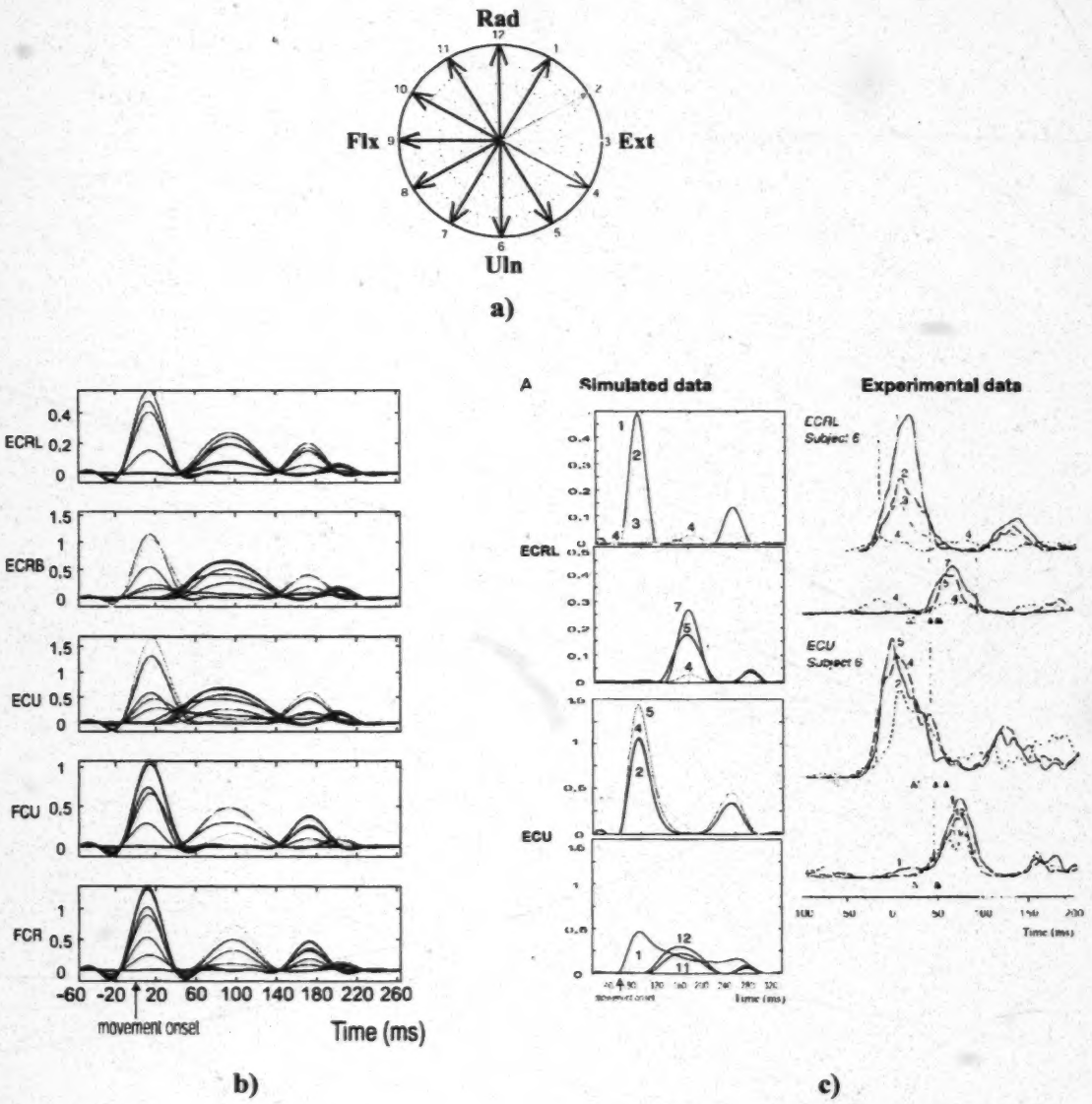

Fig 2.10: Muscle activation patterns during wrist movements. a) Target directions represented by different colours. b) Simulated EMG of the five wrist muscles, note the characteristic agonist bursts or single antagonist burst depending on the directions of the movement. c) Comparison of experimental and simulated EMG for a few targets for the ECRL and ECU muscles, the relative ranking, in terms of peak activation magnitude, for the different target directions are the same in both cases, though the shape of the activation peaks are not always similar (Haruno & Wolpert, 2005).

Thus in addition to predicting the characteristic features in the kinematics of human arm and eye movements, the minimum variance theory also predicts the unique muscle

activation patterns of wrist movement, thereby adding further support for the idea that the nervous system may adopt such a strategy for motor planning.

2.5 Signal Dependent Noise

2.5.1 Defining SDN

Mathematically, SDN is designated as a zero-mean fluctuation, the amplitude of which increases with the mean of the signal that it is corrupting. The standard deviation (SD) of the oscillation about the mean signal would be one quantitative measure of the noise amplitude. The following is an idealized illustration of a clean signal corrupted by SDN.

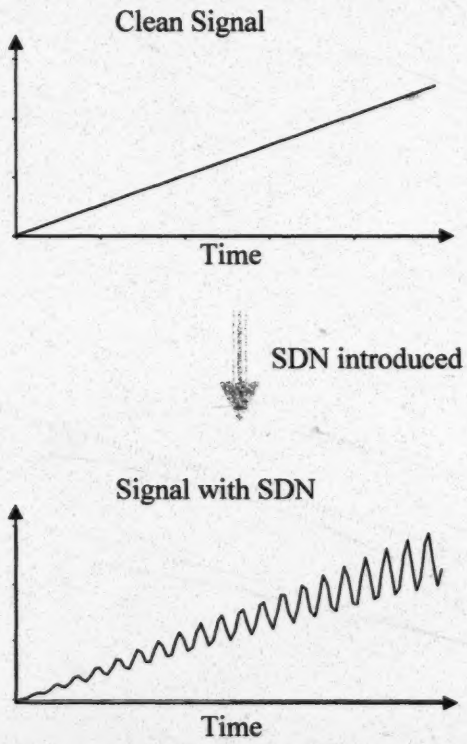

Fig 2.11: Idealized SDN. Zero mean oscillation about a mean signal. Magnitude of oscillation increases with magnitude of the mean signal.

With respect to motor control and the minimum variance theory, the SDN of interest is a physiological noise that corrupts the motor command somewhere along the descending motor pathway, which leads to undesired variability in the motor output. The disruptive effects of the SDN on the motor output can be observed in various forms: when contracting a muscle, the fluctuations in the force output increases monotonically as the mean level of the force output increases (Schmidt 1979); when making directed movements, the accuracy of the movement end point decreases as the amplitude of the movement increases (Fitts 1954). It is the SDN observed in the force fluctuations that is of primary interest to this project, the reasoning for which will be explained in the subsequent sections.

To produce a movement or a muscular contraction, control signals are generated from higher centers in the CNS and transmitted through a cascade of neural elements along the motor pathway before being converted to a force output at the muscles. In their proposal of the minimum variance theory, Harris and Wolpert did not specify the exact identity of the motor command that was corrupted by the SDN; it can therefore be interpreted as any of the signals in the signal cascade along the descending motor pathway. Due to the abstract nature of this motor command, the origin of the SDN is also somewhat ambiguous. It could originate from anywhere upstream in the nervous system or even from the activities of the muscles themselves. Moreover, there could be multiple sources of SDN corrupting the motor command at various points along the motor pathway, and the noise observed in the final motor output in this case, would be a cumulative effect of all these sources (Fig. 2.12).

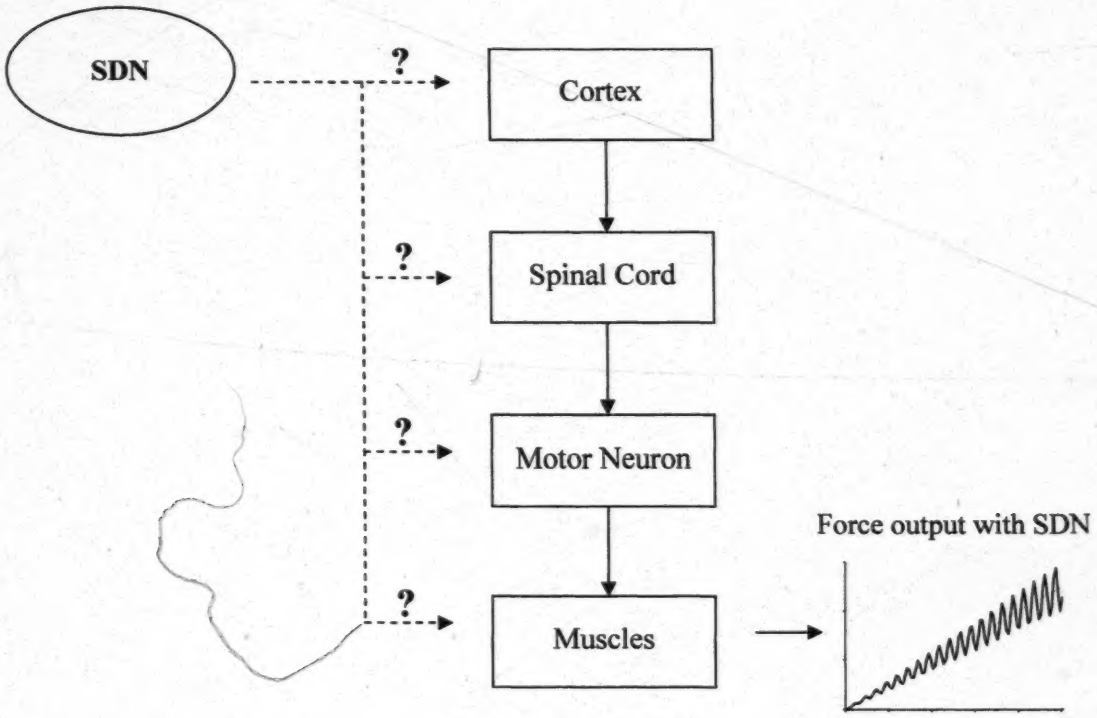

Fig 2.12: SDN in the motor system. There could be many sources of SDN that combine to produce the SDN seen in the final motor output.

2.5.2 Relevance of SDN

In performing our daily tasks, we execute various directed movements such as reaching to grab a coffee or pushing an elevator button, for which the accuracy of the movement is critical to the successful completion of the task. However, with the SDN corrupting the motor commands, such accuracy in the final motor output cannot always be guaranteed. Thus, in planning out the required trajectory of a movement, the nervous system must somehow compensate for the SDN.

In fact, the minimum variance control strategy proposed by Harris and Wolpert (1998) suggests that in the planning of a movement, the primary objective of the nervous system is to minimize the disruptive effects of SDN on the final motor output, or in other words, to make the movement as accurate as possible in the presence of the noise. Furthermore, it was assumed that this SDN scaled linearly with respect to the mean motor command, even though there was no experimental evidence to support such an assumption.

As such, a more detailed understanding in the properties of the SDN may provide evidence to support or challenge the proposed minimum variance control strategy, which may offer insight into the possible means by which the nervous system accommodates for the disruptive effects of SDN to consistently make accurate movements. Furthermore, knowledge of the SDN in normal healthy people may also contribute to the understanding of the mechanisms of various conditions during which precision of movement deteriorates and the disruptive effect of the SDN on the motor output is amplified, such as during Parkinson's disease.

2.5.3 Origin of SDN

Although in their original proposal of the minimum variance model, Harris and Wolpert hinted that the motor command of interest could be represented by motor neuron discharge rate and the corrupting SDN would thus correspond to the variability in the discharge rate, they did not make this an explicit assertion or provide any concrete evidence.

In theory, the SDN in the motor output could originate from anywhere upstream in the motor pathway: in the cortex, the spinal cord, the motor neurons, or even from the muscles themselves. In fact, a noise that increases as the mean signal increases has been observed in the discharge rate of cortical neurons (Dean et al, 1981; McAdams & Maunsell 1999) as well as the lower motor neurons that directly innervate the muscles (Clammam et al, 1969; Matthews et al, 1996, Stein et al, 2005), though the two are not necessarily related.

However, the scaling of these noises with respect to their corresponding mean signals appears to differ significantly from the scaling of the noise in force output, though uncertainties regarding the true scaling of noise over the entire range of force output remain. The scaling of the force SDN will be discussed in more detail in the following section. The discrepancy in scaling suggests that the noise in motor output cannot be the direct result of variability in the final neuronal signal along the motor pathway alone, but rather, must be a summed effect of this variability and other factors.

In 2002, a study by Jones et al (2002) set out to uncover the source of the SDN in muscle force output. The authors implemented a model of a motor unit pool based on the Fugelvand model (Fugelvand et al, 1993). The model receives an input signal that represents the descending motor drive, from which a prediction of the force generated by the pool at the given level of motor drive is computed. By varying the order in which the motor units within the pool are recruited (Fig 2.13), it was shown that the orderly recruitment of the motor units is a critical factor in determining the scaling of the noise in

the force output with respect to the force mean. Specifically, only under orderly recruitment conditions was the model able to produce a scaling in the oscillation of the predicted force output that was similar to the scaling obtained from experimental force data (Fig 2.13 c). Moreover, the simulations also showed that while variability in motor neuron discharge rate contributed to the overall amplitude of the force noise, it did not affect scaling.

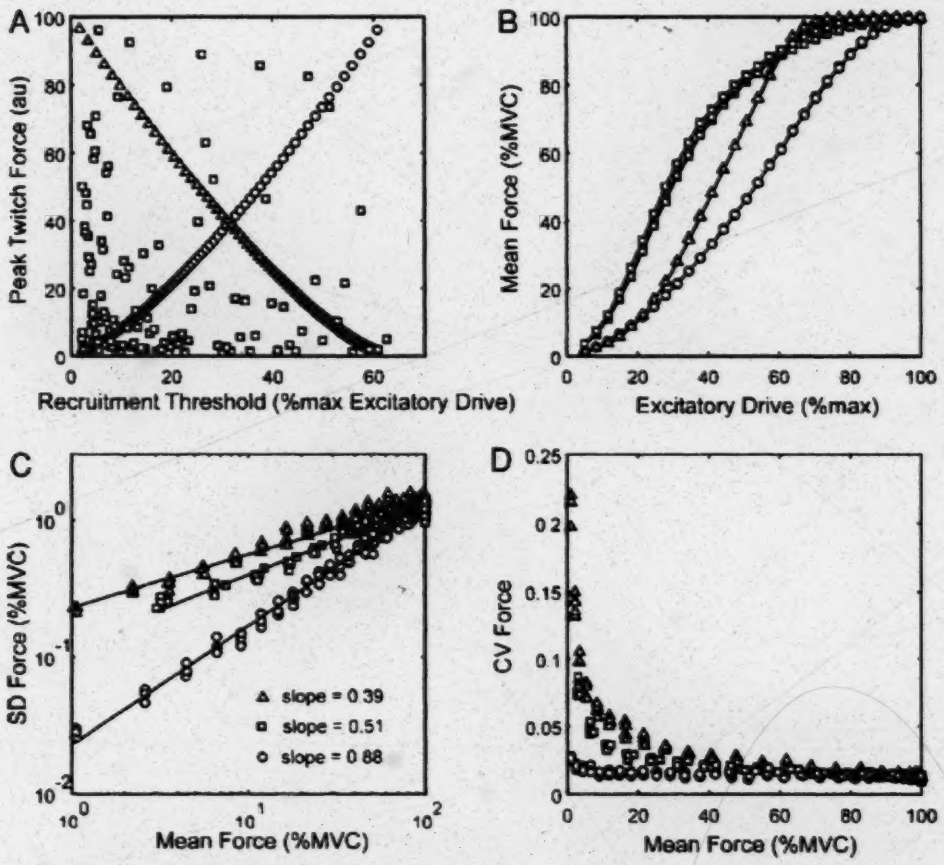

Fig 2.13: Motor unit pool simulations with different recruitment orders. a) Three recruitment orders, orderly (**O**), random (□) and reverse(Δ); b) Force output as function of excitatory drive; c) Mean vs SD; d) Mean vs CV (Jones et al 2002).

In the same study by Jones et al (2002), force output from the extensor pollicis longus muscle (EPL) in human subjects, generated from voluntary contractions as well as contractions induced by Neuromuscular Electrical Stimulation (NMES), were recorded. From this data, it was shown that while voluntary contractions produced a force output for which the SD increased as the mean increased, the two quantities were independent in the force produce from NMES induced contractions (Fig 2.14).

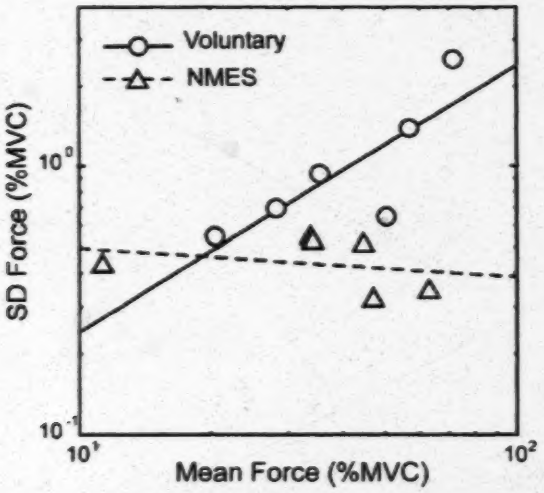

Fig 2.14: Voluntary and NMES induced contractions. Plotting SD of force vs. mean force in log-log scale, data from voluntary contractions produce a regression line with a slope of ~1, which indicates a linear relationship (Jones et al, 2002).

The authors attributed this observation to the random recruitment of motor units that occurred when muscles are excited through surface electrical stimulation. Supporting evidence for this hypothesis was provided through simulations performed using the motor unit pool model. The original model was modified such that, as the excitatory drive was increased, the motor units within the pool were recruited in random order with no regards to their twitch force amplitude. While the simulation results for the random recruitment

case did not produce a force for which the SD was completely independent of the mean, the scaling of the relationship between the two quantities was not as strong as in the orderly recruitment case, as shown by a smaller slope in a log-log plot of mean force vs. SD of force (Fig. 2.13 c).

In addition to demonstrating the importance of recruitment order in determining the properties of the noise in the force output, Jones et al also showed that variability in motor neuron firing, while having no affect on the scaling of the noise in the force output, did have an influence on the absolute level of the noise. This provides evidence that the final form of the signal dependent noise could be a result of multiple factors.

Although the exact physiological origin of the SDN in the neuromuscular system and its properties are not entirely clear, the final output of the motor system (force, movement) may provide an indirect means of observing the noise. If the muscles were simple and faithful transducers of the neural motor command, which they are not, then the fluctuations observed in force output of muscles during various types of contractions would be accurate representations of the noise corrupting the motor command.

2.5.4 Characterizing SDN

As mentioned previously, the muscles driven by the motor commands are modeled as simple linear systems in the simulations performed by Harris and Wolpert, which is in contrast to the complex behaviour of real muscles, they do not alter the nature of the SDN corrupting the motor commands when they transform these commands to force. Thus, the

SDN observed in force maybe viewed as being representative of the SDN that is of critical importance in the minimum variance model.

There have been numerous studies performed to characterize the SDN found in force output from muscle contractions. Through experiments with human subjects, Jones et al (2002) showed that the force output produced during static isometric contractions exhibited a noise that increased with the level of mean force produced. Moreover, by calculating the slope of the regression line obtained from SD and mean force data in log-log scale, it was determined that the scaling between the two variables was linear. It should be noted that the contractions performed in this study did not include the lower force range below 20% MVC. Thus, the linear scaling of the SDN observed here does not necessarily extend over the complete range of force produced from voluntary contractions.

The linear scaling in the SDN observed in the Jones study provided some support for the assumption made by Harris and Wolpert. However, as previously mentioned, the contractions performed did not cover all levels of intensities. Furthermore, a number of other studies have provided evidence to suggest that the SDN in force output may not be linear at all.

A study by Moritz et al (2004) obtained data on the force SDN over a wide range of force levels, including the lower levels that were absent in the Jones study. The study showed that the CV of the force noise actually decreased, in an exponential fashion, as the mean

force increased, at low levels of force output (Fig 2.15). This decreasing CV corresponded to a non-linear scaling between the SD and the mean of the force output. However, at intermediate to higher levels of force output, the CV was relatively flat, which represents an approximately linear scaling of the SDN in these segments, as was shown in the Jones study. Note that a decreasing CV would correspond to an SD that increases at a rate that is below linear proportions with respect to the mean force.

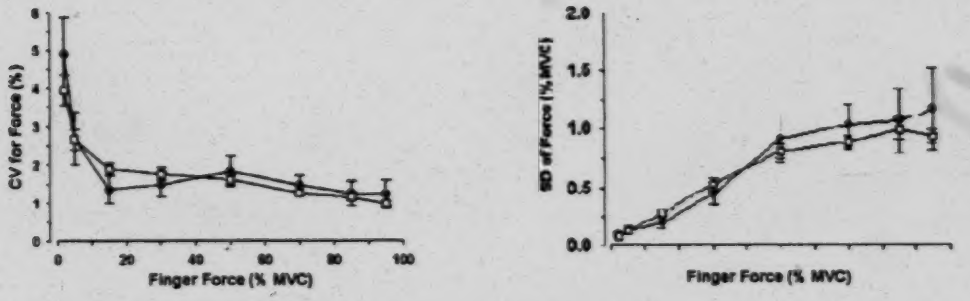

Fig 2.15: Force CV and SD (Moritz et al, 2004).

On the other hand, a study by Slifkin and Newell (1999) performing a similar set of static contraction experiments, obtained a force output with an SD that increased exponentially with respect to the mean force (Fig. 2.16). This corresponded to an increasing CV of the force noise and was not in agreement with the linear scaling observed in the Jones study, or the decreasing CV of the Moritz study.

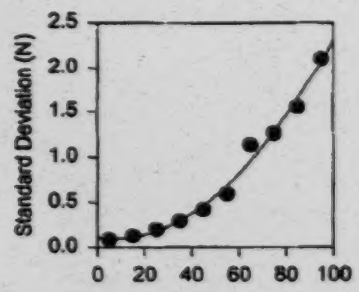

Fig 2.16: Force SD vs mean force (Slifkin and Newell, 1999)

Thus, the experimental data on SDN obtained from the Moritz and Slifkin studies were not in agreement with the linear SDN assumption made by Harris and Wolpert. Furthermore, the force outputs in the aforementioned studies were all produced from contractions performed under static isometric conditions. In real-life, movements tend to involve muscle contractions that are more dynamic and isotonic in nature.

2.6 Project Goals

The minimum variance model proposed by Harris and Wolpert is a promising theory in the search for the optimization strategy used in the nervous system to plan movement trajectories. Its power lies in the fact that it offers a unifying theoretical framework that can provide an explanation for the underlying cause of the various stereotyped features observed in human movements, in contrast to other models that simply imitate the empirical data.

However, as the accurate predictions of the minimum variance model are generated with the assumption of a linearly scaling SDN, determining the true nature of the SDN can provide validation for the minimum variance theory as a strategy employed by the CNS in planning movement trajectories. On the other hand, an SDN that does not scale linearly with the mean signal, on its own, does not necessarily disprove the minimum variance theory. The possibility that an SDN with a non-linear scaling could actually improve the

predictions of the control strategy should not be excluded. Nevertheless, characterizing the SDN in the motor system through experimental data would be very informative.

Previous studies providing data on the scaling of the SDN were all conducted under static isometric conditions, which is not representative of real life movements. However, force generated during dynamic isotonic contractions is not directly measurable. Nevertheless, characterizing the force SDN during dynamic isometric contractions may still be very informative in validating the minimum variance model. Thus the first goal of this project is to determine if the SDN in force output generated during dynamic isometric contractions differs from the SDN of static contractions. A different SDN could indicate different mechanisms behind the execution of the two types of contractions, which might require different optimization strategies.

With a number of studies providing evidence that SDN in force output generated from static contractions may not scale linearly with the mean force level, particularly at lower force levels, the second goal of this project is to establish the relationship between the SDN and mean force over the entire range of force output, for both dynamic as well as static contractions.

Upon completion of the second project goal, if it is found that the SDN does not scale linearly with mean force, as was assumed in the original Harris and Wolpert (1998) study as well as the Haruno and Wolpert (2005) study, then a mathematical description of the relationship obtained from experimental data will be derived, which will provide an SDN

that more accurately represents the empirical data to be implemented in the minimum variance model. Consequently, the effect of such a non-linear SDN on the minimum variance model's prediction of movement trajectories and muscle activation patterns can be examined. This will be the third major goal of the study. To summarize, the three main goals of this project are:

1) Determine if dynamic contractions produces SDN in force output that differs from the SDN that has been observed in static contractions.

2) Characterize the behaviour of the SDN as the mean force output is increased, thus determining the scaling of the SDN, for static as well as dynamic contractions.

3) If the scaling of the SDN is not linear as was assumed by Harris and Wolpert, then determine whether or not the observed SDN affects the predictive capabilities of the minimum variance control strategy.

3 Methods

3.1 Data Collection

3.1.1 Subject Recruitment

A total of 8 subjects were recruited for the study. The average (± SD) age of these subjects was 27 ±3. Only right handed subjects were recruited to maintain a consistent experimental setup and eliminate any differences in handedness as potential influencing factors. All subjects were screened for neurodegenerative diseases as well as previous physical trauma to the right arm or wrist, as such conditions may interfere with normal mechanisms of motor control. This was accomplished through a questionnaire which was filled out by each subject prior to the experiment.

3.1.2 Experimental Setup

At the start of the experiment, the subjects were seated in a comfortable position with their right forearm and wrist stabilized by a supporting apparatus. The forearm was restrained against the apparatus with an elastic bandage to restrict movement about the elbow joint. The subjects were then instructed to try to contract only the First Dorsal Interosseous (FDI) muscle while keeping the other muscles of the arm and hand as relaxed as possible during their contraction tasks to isolate the force output of the FDI. To measure the force generated by the FDI, a force transducer was placed perpendicular to

the right index finger, in direct contact with the proximal interphalangeal joint. This configuration measured only the force applied in the horizontal plane.

3.1.3 Data Acquisition

An Omega "S" type force transducer was used to measure the force exerted from the subjects during their contraction and output the quantity as an analog voltage. A CED 1401 micro data acquisition board digitized the analog force signal for storage on a computer. The analog data was sampled at 2000 Hz.

3.1.4 Experimental Protocol

For the first task, each subject performed three maximum voluntary contractions (MVC). The subjects were asked to simply apply as much force as possible against the force transducer using only the FDI muscle of the right hand. Each MVC was held for 3 seconds, throughout which the subjects were given verbal encouragement. A 30 second break was given between each maximal contraction. From each trial, 0.2 s (100 samples) of the highest data points, not necessarily contiguous, was extracted. The maximal data extracted from all the repetitions are then averaged to obtain an estimate of the MVC. Once the MVC value was obtained, it was used to normalize all other force recordings. After completing the MVC contractions, each subject was required to perform three different sets of isometric contractions (Fig 3.1): fast dynamic ramp, slow dynamic ramp and static. The order in which the sets were performed was randomized on a per subject basis. The slow dynamic set consisted of 10 dynamic ramp contractions with the target

force increasing from 0% to 33% MVC in 10 seconds. The fast dynamic set of contractions was similar to the slow dynamic set, only faster in rate of increase in the force: 10 ramp contractions from 0 – 66% MVC in 10 seconds. To avoid force fluctuations caused by the visual feedback loop, all contractions were performed without visual feedback. As such, all subjects were given training for the dynamic ramp contractions before actual recordings began (see next section). The last set of contractions was composed of 14 subsets of static isometric contractions, 6 at low force levels (3-15%MVC) and 8 at the intermediate to high range (20-90%MVC). Three repeat trials were performed at each of the static force levels. For each trial, the subject was given the initial two seconds to reach the designated target force with the aid of visual feedback, after which the visual feedback was taken away and the subject was required to maintain the level of contraction for the next 3 seconds. The order in which the target force levels were presented in the static contraction set was randomized for each subject. Additionally, 5 minute breaks were given prior to the start of each set of contraction while 30 second break were given between contractions within each set to avoid fatigue.

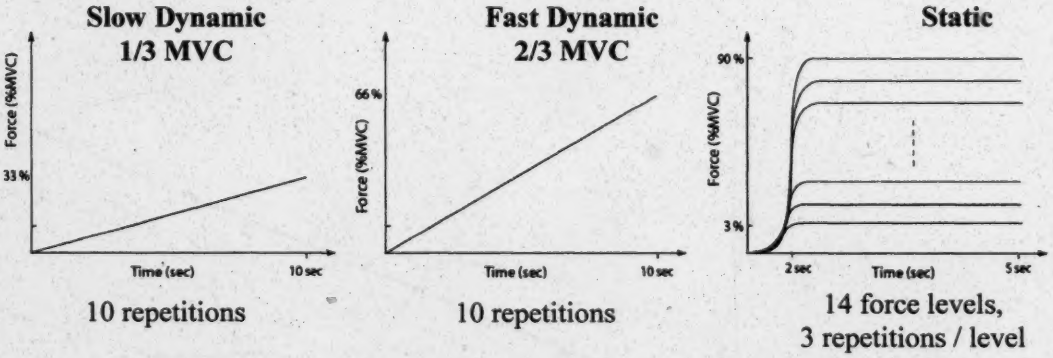

Fig 3.1: Experimental protocols for the thee types of contraction

3.1.5 Training

In order to eliminate possible undesired force fluctuations introduced by the visual feedback loop, all recorded contractions were performed without any real-time visual feedback of the actual force output. As such, prior to each set of dynamic contractions, all subjects were given training for the particular task with the aid of visual feedback. This visual feedback was provided via the Spike software on a computer screen (Fig 3.2), which displayed a real-time plot of the actual force produced by the subject against a background grid that indicated the desired target forces at various points in time.

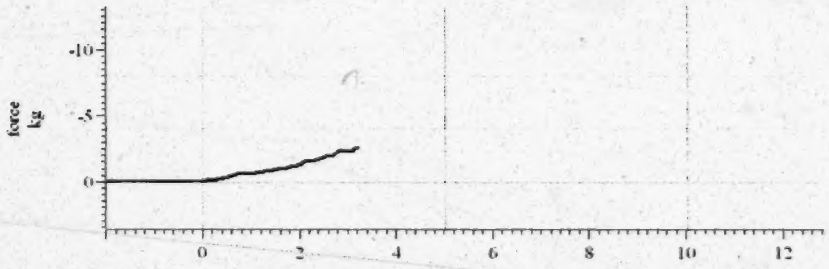

Fig 3.2: Screen shot of spike2 during training

Gradually, the visual feedback was removed by asking the subject to look away from the screen but checking back intermittently, and eventually not at all. Once the experimenter deemed, through qualitative inspection, the subject to be capable of performing a ramp contraction that was reasonably close to the ideal linear ramp, then the actual recordings began.

3.2 Data Analysis

3.2.1 Pre-Processing

As the relative strength of the FDI muscle may vary considerably between subjects, their force output is not directly comparable in absolute terms. Normalization of the force data to the maximum voluntary force output (MVC) of the particular subject allows for analysis of the force data in terms of %MVC, which may be seen as a measurement of relative effort and is thus more comparable across subjects. To determine the MVC force level for each subject, 0.2 second (100 samples at 2 kHz sample rate) worth of the highest valued, non-contiguous sample points from each of the three MVC recordings were gathered and averaged. Once the MVC value was obtained for a subject, all other raw force data recorded for that subject was normalized to the MVC such that any subsequent analysis of the force data was performed in terms of %MVC.

Prior to the analysis of the force data from the three different sets of contractions, specific information of interest was extracted from the recordings. To accomplish this, the data from each recorded contraction was divided into 1 second epochs. The mean force level of each epoch was computed. Then, a second order polynomial trend removal was applied to the epochs to eliminate the effects of intentional increases in the force output during dynamic ramp contractions, as well as any low frequency drift which are especially apparent during static contractions. From each de-trended epoch, the standard deviation (SD) was obtained, which measures the level of the SDN at the particular epoch (Fig 3.3). Moreover, the coefficient of variation (CV), which is equal to the standard deviation divided by the mean, was calculated from each mean and SD pair. Thus, for

each 1 second epoch of data, a mean force level and a corresponding CV is extracted and stored for further analysis.

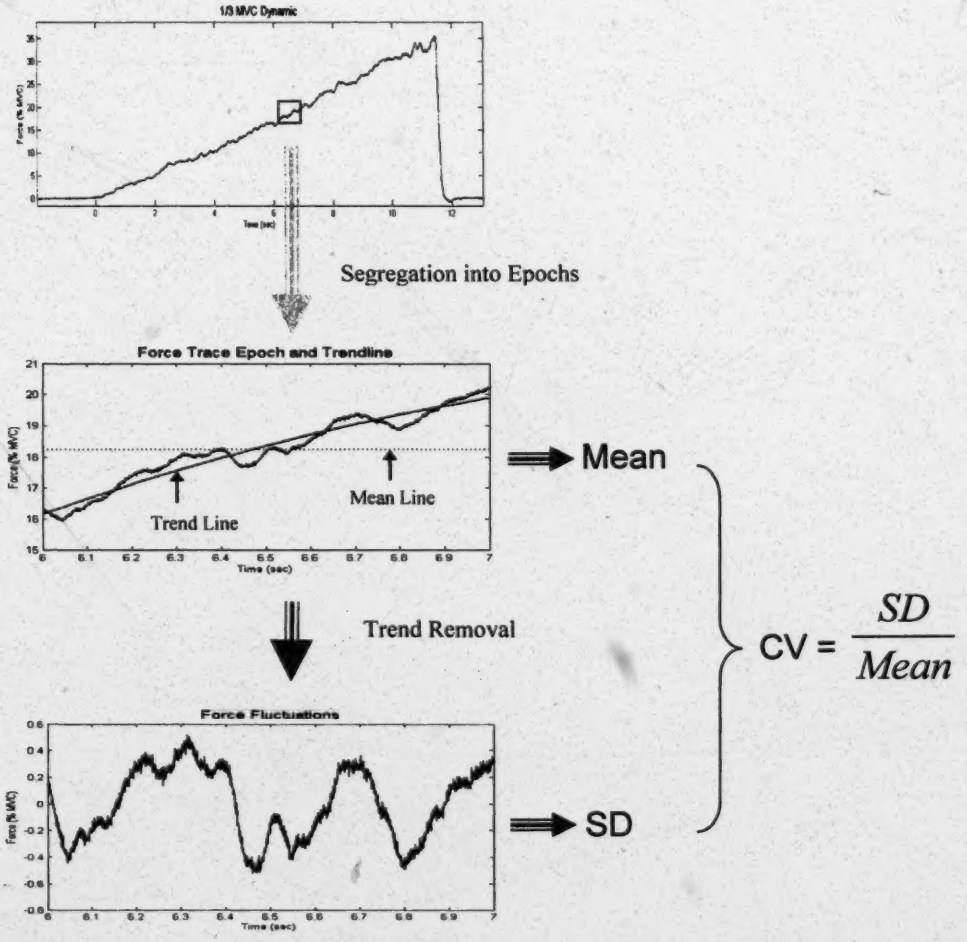

Fig 3.3: Processing of raw data. Data was divided into 1 second epochs, detrend the force data in each of the epochs, then calculated the mean and SD of the detrended force, CV is calculated as SD/mean.

Once a mean and CV pair were extracted from each available epoch, each data pair was then assigned to a force level bin according to the value of the mean force (Fig 3.4). The width of the bins was 5% MVC each, with the first bin starting at 0-5% MVC. Such

binning of the data allowed for comparison of noise levels across subjects and contraction types at equivalent force levels, thereby eliminating the mean force output as an influencing factor in the comparisons.

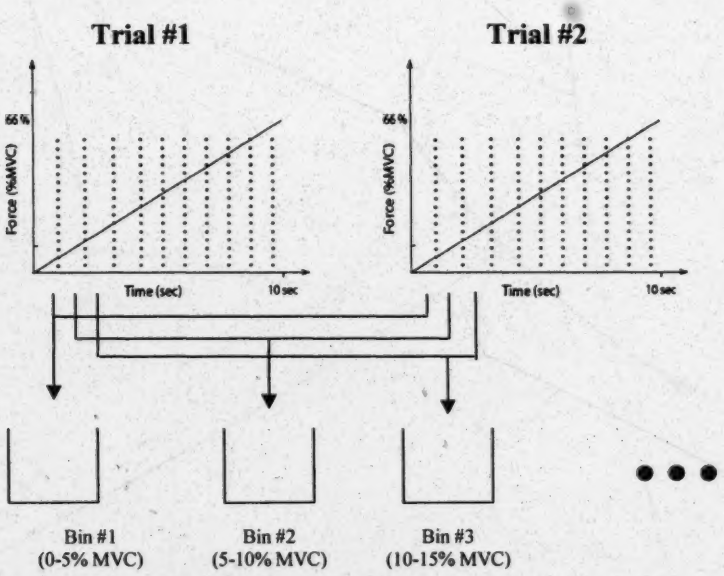

Fig 3.4: Force binning. CV data binned according to the mean force produced to allow comparison of CVs across contraction types at comparable force levels.

3.2.2 Hypotheses Testing

The goal of this project was to address the three following questions: 1) Is the signal dependent noise (SDN) different between dynamic and static contractions, or between dynamic contraction of different speeds; 2) Does the SDN vary linearly with the mean force level (i.e. constant CV) through the entire range of force outputs during voluntary contractions, as was assumed in the Harris and Wolpert (1998) study?; and 3) if the SDN

indeed has a non-linear relationship with the mean force, does this have any significant impact on motor control and the achievement of accurate movements?

Scaling of SDN

A plot of the CV against the mean force provided a qualitative method for ascertaining the scaling of the noise amplitude with respect to the mean force output. Since the CV was just the SD of the force output divided by the mean, a constant CV over the entire force range would indicate a linear relationship between the mean and the SD. However, the CV plot revealed that the CV was clearly not a constant line but rather, decayed in an exponential fashion as the mean force increased. As such, a mathematical model of the form $CV_{min} + (CV_{max} - CV_{min})e^{-u(t)/\tau}$ was fit to the data using the least square method to obtain a quantitative description of the CV for the SDN. The parameters CV_{max} and CV_{min} were the maximum (at 0%MVC) and minimum (at 100%MVC) values of CV, and κ was the constant that determined the rate at which the CV decayed as the mean force increased.

Influence of Contraction Type on SDN

To determine whether the SDN is affected by the type of contraction made, all the data pairs (mean and CV) were separated according their contraction type (ie dynamic fast, dynamic slow, static). A one way Analysis of Variance (ANOVA), accounting for random effect of inter-individual variation and using a significance level of $p < 0.01$, was performed for each of the force bins, with contraction type as the sole factor. This

analysis determined whether the mean CV values, at comparable force levels, differed significantly when various types of contractions were performed.

Effect of Non-linear SDN on the Minimum Variance Model

To determine if a non-linear SDN (i.e. non-linear relationship between force SD and mean) would affect the movement planning using the minimum variance strategy, such a non-linear noise was implemented in the wrist model developed by Haruno (2005). For a more detailed description of the model, see the section below. Previously with the linear SDN, the cost function to be minimized was:

$$\sum_{i=1}^{5} \int_{M}^{M+P} \int_{0}^{t} CV_{const}{}^{2}\ u_i{}^{2}(\kappa)\ p^2(t-\kappa)\ d\kappa\ dt \tag{3.1}$$

Since the CV term was constant, it was pulled out of the summed integral to simplify the calculations:

$$CV_{const}{}^{2} * \sum_{i=1}^{5} \int_{M}^{M+P} \int_{0}^{t} u_i{}^{2}(\kappa)\ p^2(t-\kappa)\ d\kappa\ dt \tag{3.2}$$

If a non-linear SDN was introduced to the model, then the cost function becomes:

$$\sum_{i=1}^{5} \int_{M}^{M+P} \int_{0}^{t} CV(u_i)^2\ u_i{}^{2}(\kappa)\ p^2(t-\kappa)\ d\kappa\ dt \tag{3.3}$$

The non-constant CV term must now stay inside the integral, adding complexity to the optimization problem. For an approximation of the CV, the mathematical equation fit to

the experimental CV data was applied to the equation, which changed the cost function to:

$$\sum_{i=1}^{5} \int_{M}^{M+P} \int_{0}^{t} \left[CV_{\min} + (CV_{\max} - CV_{\min}) e^{-\frac{u_i(\kappa)}{MVC_i}/\tau} \right]^2 u_i^2(\kappa)\, p^2(t-\kappa)\, d\kappa\, dt \qquad (3.4)$$

where MVCi is the maximal motor command that can be achieved by muscle i under MVC conditions. Finding an optimal solution to this equation would require the use of constrained, non-linear optimization methods. Unfortunately, we did not have the expertise in this area to achieve this task with confidence, and have thus left it for future work.

Instead, we used the motor commands optimized for a linear SDN, and applied Gaussian noise with either a constant or a non-linear CV. The resultant wrist trajectories were then computed for the center-out task. By comparing the trajectories generated with the two types of noises, we could determine whether the non linear noise had a significant effect on the movement.

The non-linear noise was characterized by the curve fitted to the fast dynamic contraction data, which had the highest CV (see Results). However, while the fitted CV curve was specified in relative terms of normalized mean force, the model motor command term u_i in the cost function of the model was provided in absolute terms of arbitrary units. As such, the model motor command must be converted to relative terms (%MVC) so that it would be comparable to normalized mean force. However, this required an MVC value

for the model motor command which could not be accurately obtained, as it was unclear what simulation parameters (movement duration and amplitude) in the model could have generated such an MVC that would correspond to the experimental force MVC. To circumvent this obstacle, we determined the maximum activation in the motor commands for each muscle under the conditions of the original model: 20° in 200 ms (Haruno 2005). These maximal motor commands were typically observed in movements in directions that were close to the muscle's preferred direction. From this point, two alternative assumptions were made. In the first case, we assumed that a 20°, 200 ms movement is more or less the fastest movement that a wrist could realistically generate. This corresponded to assuming that the maximum motor commands obtained under these conditions were equivalent to motor commands at 100%MVC, and hence could be used directly as an estimate for the MVC motor commands. In the second case, it was assumed that the fastest wrist movements in real life were faster than the simulated condition, and that the maximum motor commands obtained under this condition were only 50% of what the motor command would have been at 100%MVC. Under this assumption, the estimated MVC motor commands would be twice the magnitude of the same estimated variables obtained under the first scenario. Consequently, the second scenario corresponded to a "high end" estimate of the CV that had a decay constant that was twice as large as the "low end" CV estimate obtained from the first scenario:

Low Estimate of CV:

$$CV_{\min} + (CV_{\max} - CV_{\min}) e^{-\frac{u_i(t)}{u_{\max 1,i}}/\tau} \tag{3.5}$$

High Estimate of CV:

$$CV_{\min} + (CV_{\max} - CV_{\min})e^{-\frac{u_i(t)}{u_{\max 2,i}}/\tau} \tag{3.6}$$

where:

$$u_{\max 2,i} = 2 \times u_{\max 1,i} \tag{3.7}$$

Simulated trajectories with the two non-linear CV's and the constant CV were computed. Thirty repeated trials were simulated to obtain a distribution of end point positions for each case. The variability of the X and Y coordinates at the end of the movements were compared for the constant and non constant CV conditions. Furthermore, a Confidence Interval error ellipse was calculated for each set of 30 simulations, thus 30 such sets were simulated to obtain a small sample of error ellipse sizes. The average size of the error ellipses under the two noise conditions were compared to determine if the non constant CV noise has a significant impact on the movement planning strategy used.

The Haruno Wrist Model

The wrist model developed by Haruno et al (2005) consisted of five muscle elements, each of which provided a pulling force on the wrist joint in a specific direction. These five muscles were all modeled as identical second order linear systems:

$$\frac{1}{(0.03 * s + 1)(0.02 * s + 1)} \tag{3.8}$$

The wrist dynamics were also modeled as a linear system:

$$\frac{1}{\left(m*s^2+b*s+k\right)} \tag{3.9}$$

with parameters moment of inertia (m), viscosity(b), and stiffness(k) chosen within a biologically plausible range. Together, these two linear systems formed the plant with an impulse response described by p(t),

$$p(t) = \mathcal{L}^{-1}\left\{\frac{1}{(0.03*s+1)(0.02*s+1)} * \frac{1}{\left(m*s^2+b*s+k\right)}\right\} \tag{3.10}$$

which determined the magnitude of the pull vector for each muscle from the input motor command u_i. Each muscle was assigned an angle (α_i), obtained from monkey experiments, that specifies the direction in which it can pull. The expected position of the wrist at any point in time was calculated by summing the pull vectors of all five muscles over a period of time:

$$E[x(t)] = \sum_{i=1}^{5} \sin\alpha_i \int_0^t u_i(\kappa)p(t-\kappa)\, d\tau \tag{3.11}$$

$$E[y(t)] = \sum_{i=1}^{5} \cos\alpha_i \int_0^t u_i(\kappa)p(t-\kappa)\, d\tau \tag{3.12}$$

This wrist model was implemented under a center out task framework, in which there were 12 evenly spaced out targets that required 20° movement of the wrist to reach. The duration of the movement was restricted to 200 ms.

Applying the minimum variance control strategy to this framework, an SDN was introduced to each u_i. Since the SDN is a zero mean noise, it does not have any effect on the average position. With the SDN, a positional variance was now present throughout the duration of the movement and can be determined by:

$$Var\,[x(t)] = \sum_{i=1}^{5} \sin^2 \alpha_i \int_0^t Var\,[u_i(\kappa)] * p^2(t-\kappa)\, d\tau \qquad (3.13)$$

$$Var\,[y(t)] = \sum_{i=1}^{5} \cos^2 \alpha_i \int_0^t Var\,[u_i(\kappa)] * p^2(t-\kappa)\, d\tau \qquad (3.14)$$

In their paper, Haruno et al (2005), assumed that the SDN scaled linearly with the mean motor command, in accordance with the Harris and Wolpert study (1998) that originally proposed the minimum variance theory. As such, the SD of the noise was described by $k\,u_i(\tau)$, where k is the CV of the noise, and $Var[u_i(\tau)]$ is simply the SD squared. Thus applying the minimum variance strategy, where the goal is to minimize the positional variance during a post movement period while still reaching the target at the end of the movement period, the cost function to be minimized was described as follows:

$$\sum_{i=1}^{5} \int_{M}^{M+P} \int_{0}^{t} CV_{const}^{\,2}\; u_i^{\,2}(\kappa)\; p^2(t-\kappa)\, d\kappa\, dt \qquad (3.15, \text{same as } 3.1)$$

where M is the movement period, P is the post movement period during which positional variance is to be minimized, and $CV_{const} = k$. Finding the u_i's to minimize this cost function would thus satisfy the minimum control strategy. With the linear SDN (constant CV) the cost function was minimized using the quadratic programming method of

optimization. However, if the SDN did not scale linearly with respect to the mean motor command (non constant CV), then the cost function to be minimized becomes:

$$\sum_{i=1}^{5} \int_{M}^{M+P} \int_{0}^{t} [CV(u_i)]^2 \; u_i{}^2(\kappa)\, p^2(t-\kappa)\, d\kappa\, dt \qquad \text{(3.16, same as 3.2)}$$

where the CV now varies as a function of u_i. Note that the u_i's are described in terms of arbitrary units, thus must be multiplied by an appropriate scaling factor or normalized (to MVC motor command) if they are to be compared with an actual motor command signal.

4 Results

Eight healthy young adults participated in the study. Each subject performed three sets of isometric contractions: fast dynamic, slow dynamic and static. Figure 4.1 shows the force traces from one subject.

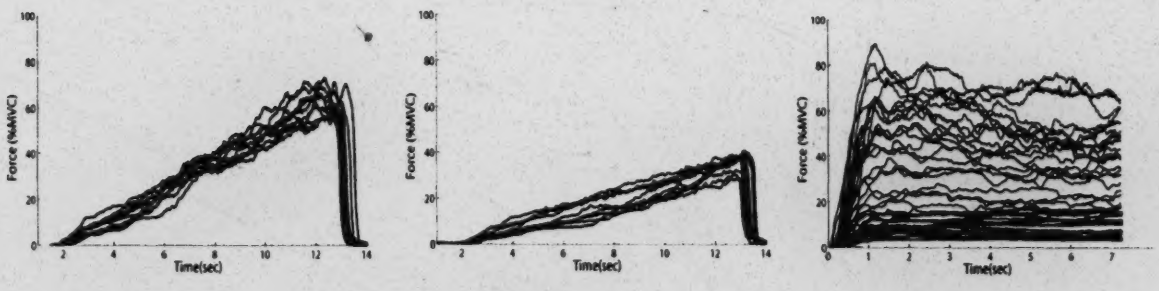

Fig. 4.1: Raw force traces. Force recordings from a single subject, during fast dynamic (left/blue), slow dynamic (center/green) and static (right/red) isometric contractions.

MVC was obtained for each subject and used to normalize the force data. The mean MVC for the group was 39.9 N (SD = 13.5 N), and ranged from 22.0 N to 58.9 N. As the contractions were performed without visual feedback, the actual force produced did not always match the ideal target exactly. The peak force reached by all subjects for the fast dynamic contractions, for which the ideal target was 66%MVC, had a mean (±SD) of 62.5±9.1 %MVC. For the slow dynamic contractions, the peak forces reached 35.6±5.3 %MVC, compared to the ideal target of 33%MVC. Each force trace was divided into 1 second epochs. A mean and standard deviation pair was obtained from each epoch along with a corresponding CV value (CV = standard deviation / mean). A scatter plot of the

CV vs the mean force is shown in Fig 4.2a, while a similar plot of SD vs mean force is shown in Fig 4.2b. These two sets of graphs are also plotted on log-log axes (Fig 4.2 c,d). From this data set, the relationship between the force noise (SD or CV) and mean force was examined.

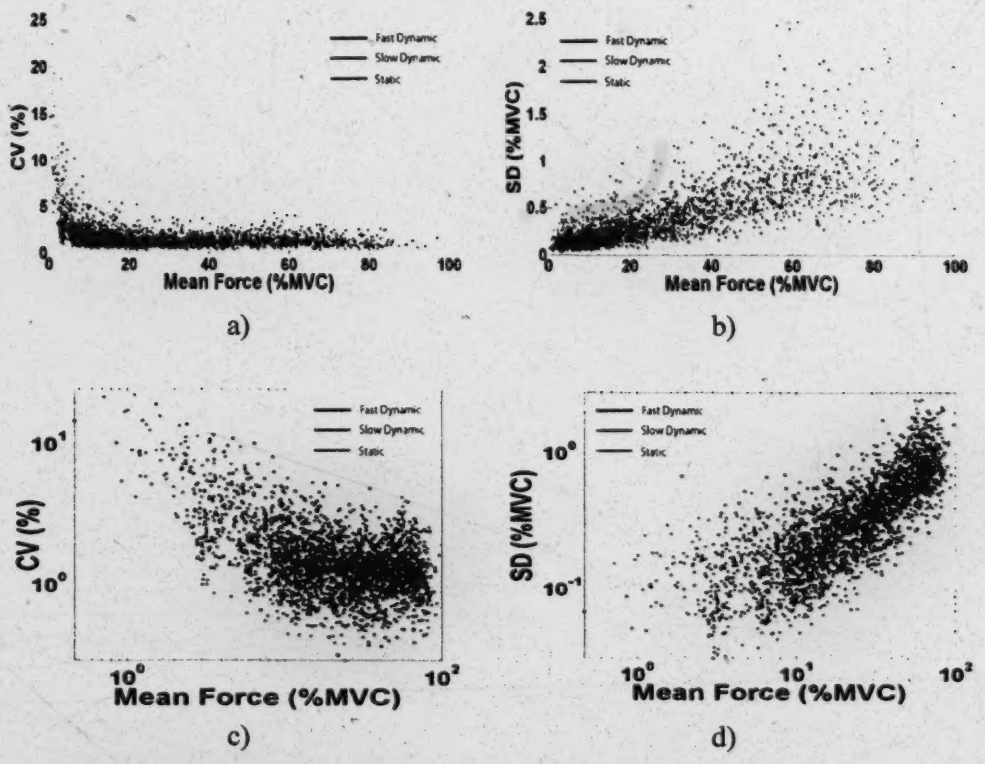

Fig 4.2: CV and SD vs mean force. CV vs Mean Force plotted on linear scale (a) and log scale (c). SD vs Mean Force plotted on linear scale (b) and log scale (d).

4.1 SDN Under Different Types of Contractions

To compare the SDN between the three types of contractions, the median and 95% confidence intervals of the force CV from each contraction group was determined and plotted (Fig 4.3). Overlapping of the confidence intervals indicate that the CV's are not

significantly different. Only data from the 8 lowest force bins (0-40%NVC) were included in the comparison because only within this force range was data available for all three types of contractions, as the ideal target of slow dynamic contractions was only 33%MVC. Furthermore, CV from fast dynamic and static contraction data remained essentially constant for forces above the 35-40%MVC bin. From figure 4.3, it could seen that the CV values tended to be highest for the faster dynamic contraction and lowest for static contraction, while the slower dynamic contraction was somewhere in between, though the differences were not statistically significant at intermediate and higher force levels, as the confidence intervals for the different contraction types all overlapped at these levels.

Repeated Measures one way ANOVA tests ($p < 0.05$) were also performed comparing the CV data across the three contraction types at each of the force bins. These tests also showed that the type of contraction had an effect on the level of CV of the force noise, but only at the force bins <15%MVC. Post hoc analysis was performed using the Tukey Least Significant Difference test on those three lower bins to reveal that the differences were only between the static and the dynamic contractions. The CV generated from the two dynamic contractions were not significantly different.

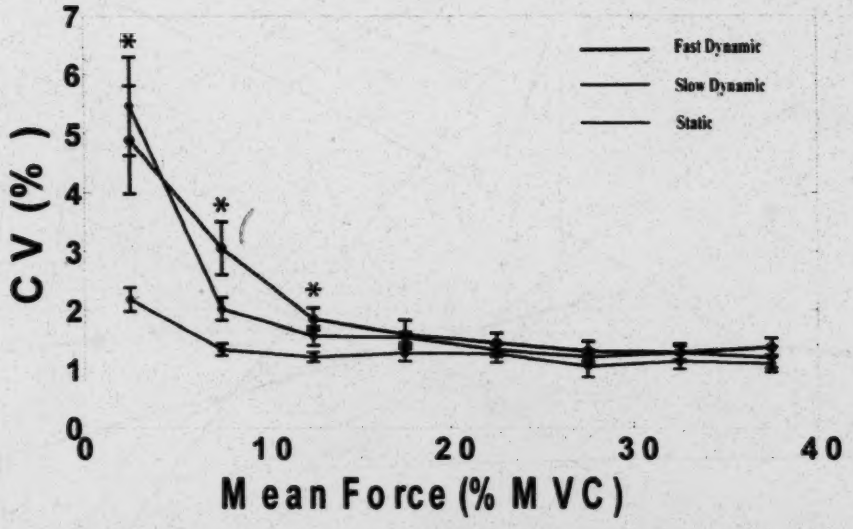

Fig 4.3: CV vs mean force. Plot of CV vs Mean Force for fast dynamic (blue) slow dynamic (green) and static (red) isometric contractions. The lines represent median values of CV while the error bars represents the 95% confidence interval. The stars above the first three bins indicate a significant difference between the CV values across the contraction types (ANOVA $p<0.05$).

Overall, the types of contraction performed in this study do appeared to have different effects on the level of noise observed in the force output. However, this difference was only significant at forces below 15%MVC, though the general trend of fast dynamic contractions producing the highest level of noise and static contractions generating the lowest noise was maintained at higher force levels.

4.2 Scaling of SDN

Having established that the different types of contractions generated different levels of noise, the next question of interest was whether or not the SD of the noise scaled linearly with the mean force. From an initial inspection of the CV vs Mean Force scatter plot in

Figure 4.2a, it seemed likely that the CV decreased as the mean force increased, in a somewhat exponential manner. The same trend was evident in the CV confidence intervals (Fig. 4.3) for all three contraction types. ANOVA tests ($p<0.01$) with bin levels as the factor confirmed that the CV values in bin #1 (0-5%) were different from the CV values in bin #5 (20-25%MVC) under all contraction types, and that the difference was statistically significant. On the other hand, the test results also showed that the CV values in bins with force levels greater than 20%MVC were not significantly different from each other. Thus, these results seemed to suggest that the CV starts at a high initial value at very low forces, and then decreases by a magnitude that is not insignificant as the force increases, before reaching a final steady state value at higher force.

Given these observations, the CV data of each contraction type was fitted separately to an equation of the form: $CV_{min} + (CV_{max} - CV_{min})e^{-u(t)/\tau}$ where CVmin, CVmax, and κ are the parameters, and u is the independent variable of mean force. The values of the fitted parameters are presented in Table 4.1 and the resulting curves are shown in Fig 4.4.

	CV_{min}	CV_{max}	τ	r^2
Fast Dynamic	0.0146	0.1103	4.3854	0.494675
Slow Dynamic	0.0155	0.2434	1.7725	0.66899
Static	0.0133	0.0472	2.6800	0.027984

Table 4.1: CV curve fitting parameters.

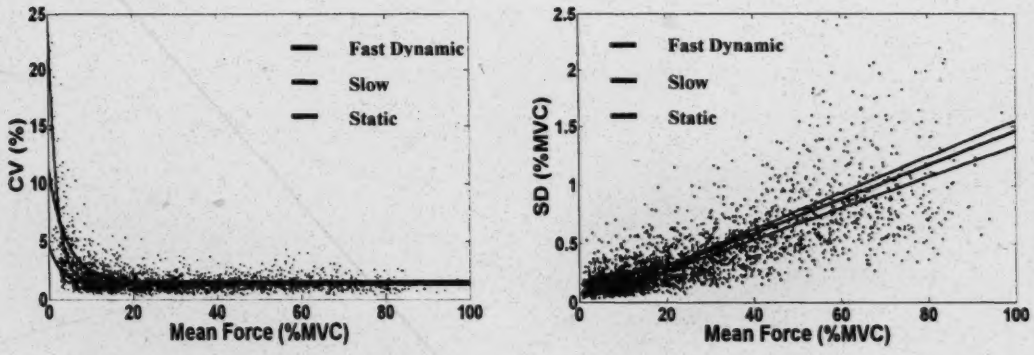

a) b)

Fig 4.4: CV and SD vs mean force. Plots of CV vs Mean (a) and SD vs Mean (b), with the three types contractions distinguished by colour. The lines are the curves fitted to the experimental CV data. The lines in b) are simply the fitted CV curves converted to SD.

The relatively low r^2 values, particularly in the case of the static data, can be accounted for by the fact that the CV data appear to be fairly constant over much of the force range, which means that an average line would make a reasonable approximation.

From the fitted curves, it can be shown that, in all three contraction types, the CV curve has undergone at least 99% of its decay and has more or less reached its final steady state value by 20%MVC, which supports the notion that the SD and mean force relationship is basically linear for force levels above 20%MVC. Moreover, there was a sizeable difference in the CVmin and CVmax parameters obtained in all three cases, which supports the idea that the CV was not constant and the mean and SD relationship was not linear over the entire range of voluntary force.

4.3 Effect of Non-linear SDN

With the knowledge that the SD of the force noise does not scale linearly with the mean force, we set out to investigate the impact that such a non-linear scaling noise would have on the predictions of the minimum variance control strategy. For this task, simulations were performed using the Haruno wrist model (Haruno 2005; also see Methods) under linear as well as non-linear noise conditions. The non-linear SDN was approximated using the CV curve fitted to the experimental data from the fast dynamic contractions. A high estimate noise and a low estimate noise were considered for the non-linear SDN case (see Methods). For the linear SDN, a noise with a constant CV that is equal to the asymptotic CV_{min} parameter of the CV equation used for the non-linear SDN was applied. The model simulated center out tasks via wrist movements. Predictions for trajectories to 12 different targets are generated, as shown in Fig 4.5a. The different noise conditions are each represented by a different colour. The confidence interval error ellipses provide a measure of the end point variability at each of the targets (Fig 4.5b). A qualitative inspection of the figure shows that the trajectories predicted under linear and non-linear noise conditions are not radically different, as in both cases, the paths are relatively straight and smooth, with a tendency to curve away from the target near the end of the movement.

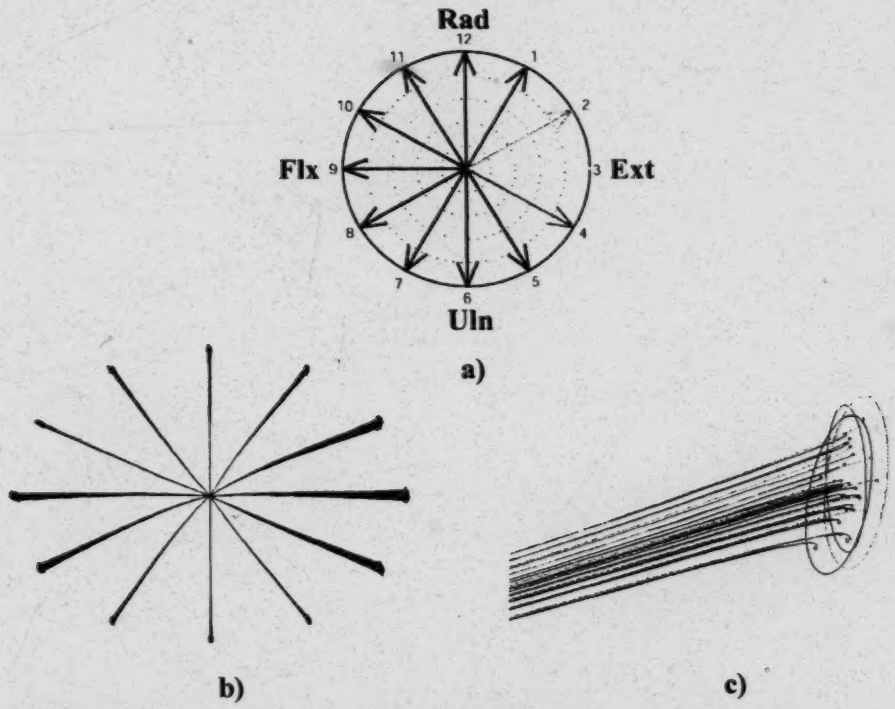

Fig 4.5: Simulated trajectories. a) target directions. b) Predicted Trajectories to 12 targets under different noise conditions, each represented by a different colour. Red = constant CV, Green = Low Estimate CV, Blue = High Estimate CV. c) Close up of trajectory end points at target 2. The terminal variability is measured by confidence interval error ellipses.

To gain a sense for the end point deviations from each target under the various noise conditions, a plot of the X coordinate and Y coordinate deviations from the ideal coordinates of each of the 12 target are plotted below (Fig 4.6). For most target directions, there is significant overlap between the confidence intervals of the deviations, which would indicate that a non-linear noise does not differ significantly from a comparable linear noise, which has a constant CV that is equivalent to the non-linear noise at high force levels. However, the most erroneous end points are typically observed in the paths produced with the higher estimate of the non-linear noise (blue line in Fig 4.6). Moreover, it seems that the largest deviations tend to occur in certain directions for both X and Y coordinates: directions 3, 4, 8, 9, and 10.

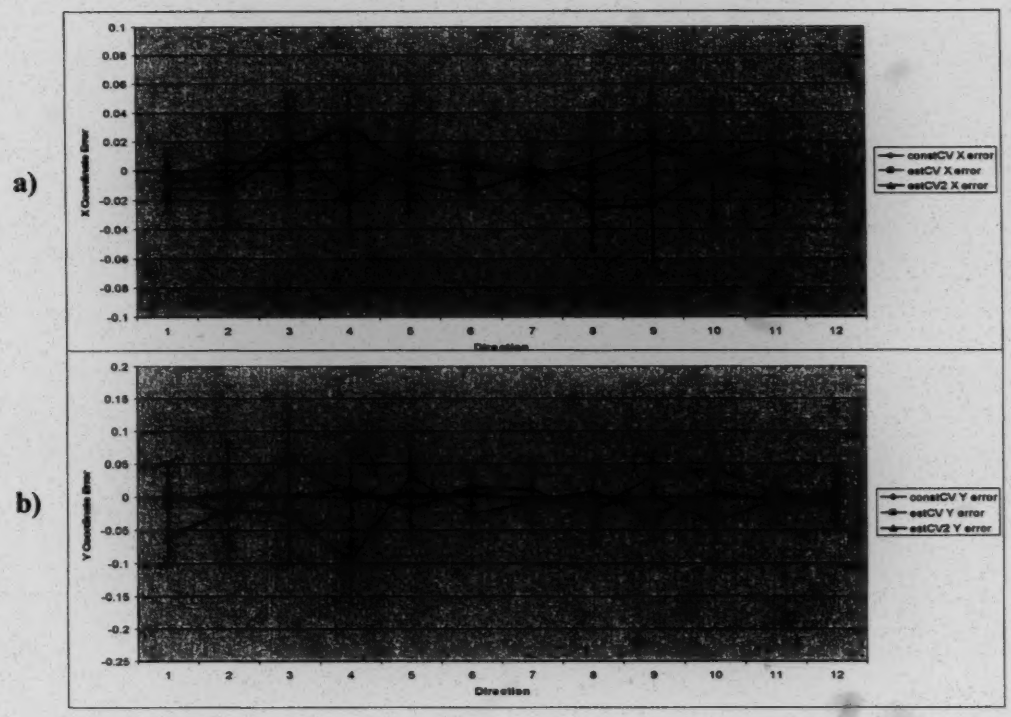

Fig 4.6: Simulated end position coordinate errors. X coordinate (a) and Y coordinate (b) deviations from target coordinates under all three noise conditions over 100 trials. The errorbars are confidence intervals.

For analysis of the error ellipses as a measure of the terminal variance, 30 sets of trajectories were simulated under each noise condition, for each of target. The polar plots in Fig 4.7 compares the error ellipse areas obtained under each of the noise conditions. Similar to the comparison of X-Y coordinate deviations in the trajectory end points presented in Fig 4.6, the non-linear noises do not affect the areas of error ellipses much differently than the linear noise. The only significant difference occurs in direction 12 and 6, which interestingly, is where absolute magnitudes of the ellipse areas are the smallest, regardless of the characteristics of the noise. Furthermore, the error ellipse with

the largest areas tend to be found in directions 3, 4, 8 and 9, which is consistent with the results obtained in Fig 4.6, thus confirming the fact that movements in these directions tend to produce the largest end point variability.

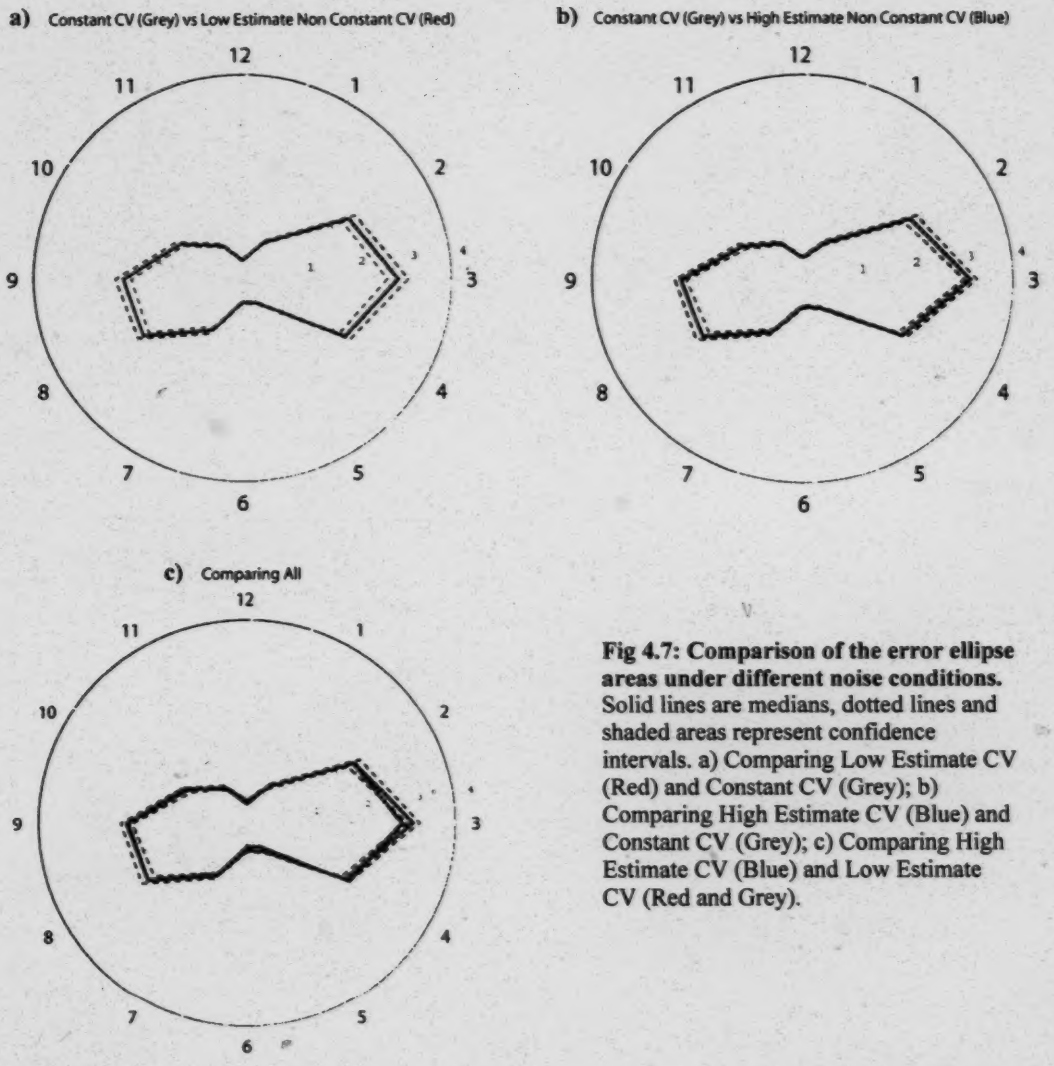

Fig 4.7: Comparison of the error ellipse areas under different noise conditions. Solid lines are medians, dotted lines and shaded areas represent confidence intervals. a) Comparing Low Estimate CV (Red) and Constant CV (Grey); b) Comparing High Estimate CV (Blue) and Constant CV (Grey); c) Comparing High Estimate CV (Blue) and Low Estimate CV (Red and Grey).

5 Discussion

5.1 Different Contraction Types Produce Different SDN

This study was the first to compare the force noise produced during dynamic contractions with those of static contractions, as previous studies of this nature focused primarily on static contractions. The results showed that, overall, the relative noise levels as measured by force CV tended to be higher during dynamic contractions than for static contractions, though the differences were only statistically significant at lower force levels (<15%MVC). This suggests that the type of contraction executed indeed has an effect on the characteristics of the noise produced in the force output, and that this effect is most evident at low force levels.

Moreover, it seemed that the fast dynamic contractions tended to produce the highest force CV, while slow dynamic contractions produced a lower CV, and the static contractions produced the lowest CV (Fig 4.3). This suggests a possible correlation between the relative speed of contraction, or potentially movement, and the relative level of the motor noise as measured by the CV. Interestingly, the motor unit pool simulations from Jones et al (2002) showed a similar increase in CV at low forces as the recruitment of the motor units deviates from orderly recruitment patterns. Specifically, under orderly recruitment conditions, the motor unit pool model generated force output with a CV that is relatively low at low force levels and decreases slightly before reaching a plateau. When the recruitment is random, the CV starts at an intermediate level at low forces, but

eventually plateaus at a similar value as in the orderly recruitment case at higher forces. However, if the recruitment order is completely reversed, then the CV starts at a level that is higher than the previous two cases at low forces before decreasing and eventually reaching a plateau similar to the other two cases (Fig 5.1 a). Figure 5.1 displays the simulated CV under various recruitment orders and the experimental CV under different contraction types together.

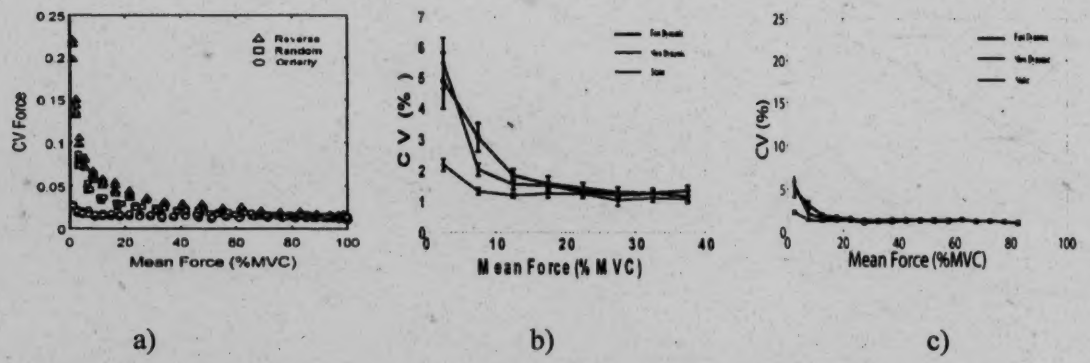

a) b) c)

Fig 5.1: Contraction speed and recruitment order. a) Simulations from Jones et al (2002) showed that deviation from orderly recruitment increases force CV. b) Experimental data shows faster dynamic contractions produce, for the most part, higher CV than slower dynamic or static contractions. c) Data displayed on same scale as (a) shows experimental CV is much closer to orderly recruitment CV than random or reversed recruitment CV.

The similarity in the increase of CV resulting from disorderly recruitment and increasing speed of contraction indicates a potential link between the two factors. Indeed there is evidence showing that disorderly recruitment can occur for faster movements or contractions. Through single unit recordings, Desmedt et. al (1979) showed that during ballistic contractions, which are very short, activation of motor units tend to occur in a burst, during which the order of recruitment for the units can be somewhat random. Essentially, during the increasing phase of any single ballistic contraction, the temporal

order in which the involved motor units are recruited can be random. However, the recruitment rank of the units still appeared orderly if the threshold is designated according to the peak force required to recruit a motor unit during separate contractions of various intensities.

In summary, contractions of different nature will tend to produce different levels of SDN. The difference is more apparent at low force levels and is likely the result of random deviations from a strict orderly recruitment of motor units.

5.2 The SDN Scales Non-linearly With Mean Force

Among the previous studies investigating SDN in force output, there had been some discrepancies with respect to the behaviour of the force CV in relation to the mean force. Harris and Wolpert (1998) initially assumed that the SD of the noise scaled linearly with the mean force in their proposal of the minimum variance theory. Jones et al (2002) provided evidence to support the linear assumption, though their data did not cover the low end of the force range. Moritz et al (2004), on the other hand, showed a non-linear noise with a CV that initially decreased at low force ranges, but then becomes relatively constant at higher force levels. The constant CV corresponds to a linearly scaling force noise, which is in agreement with the data from the Jones study in the intermediate to high force range (>20%MVC). Thus, despite the different conclusions drawn by the two groups, their results are not in conflict. However, in the Moritz data, the CV settled at approximately 1-2% at intermediate to high force levels, while the CV values at similar force levels extracted from the Jones study was higher at around 2-3% (Fig 5.2). The

overall higher CV level in the Jones data could be due to the fact that subjects in the Jones study performed contractions of the EPL muscle, while the Moritz study involved contractions of the FDI muscle. The Slifkin & Newell study also involved contractions of the FDI. The SD data obtained by this group increased in an exponential manner in relation to the mean force. This resulted in a significant upward trend in the CV at higher forces (Fig 5.2), though at low forces, the CV decreased with an increasing mean force, just like the Moritz study. The cause for this discrepancy is not entirely clear, though a partial explanation could be a difference in the method of analysis. While the other three studies normalized the data to each subject's MVC before averaging the SD or CV, Slifkin & Newell simply averaged the SD in terms of the absolute force.

The results obtained from our study were most similar to those of the Moritz study, though their static data more closely resembled our dynamic data than our static data. In both studies, the CV started at a relatively high initial value and decreases as the mean force increases. Once the mean force reaches a sufficiently high level, the CV becomes essentially constant. One feature in which our CV profile differed from the other three studies is that our CV stays more or less flat at higher force levels, while the CV from other studies all show some level of increase following the initial descent, though this secondary CV increase is not as prevalent in the Moritz data. Nevertheless, there is no disagreement among the studies regarding the initial descent of the CV at the lower force range, which means that the SD of the noise is not linear with respect to the mean force.

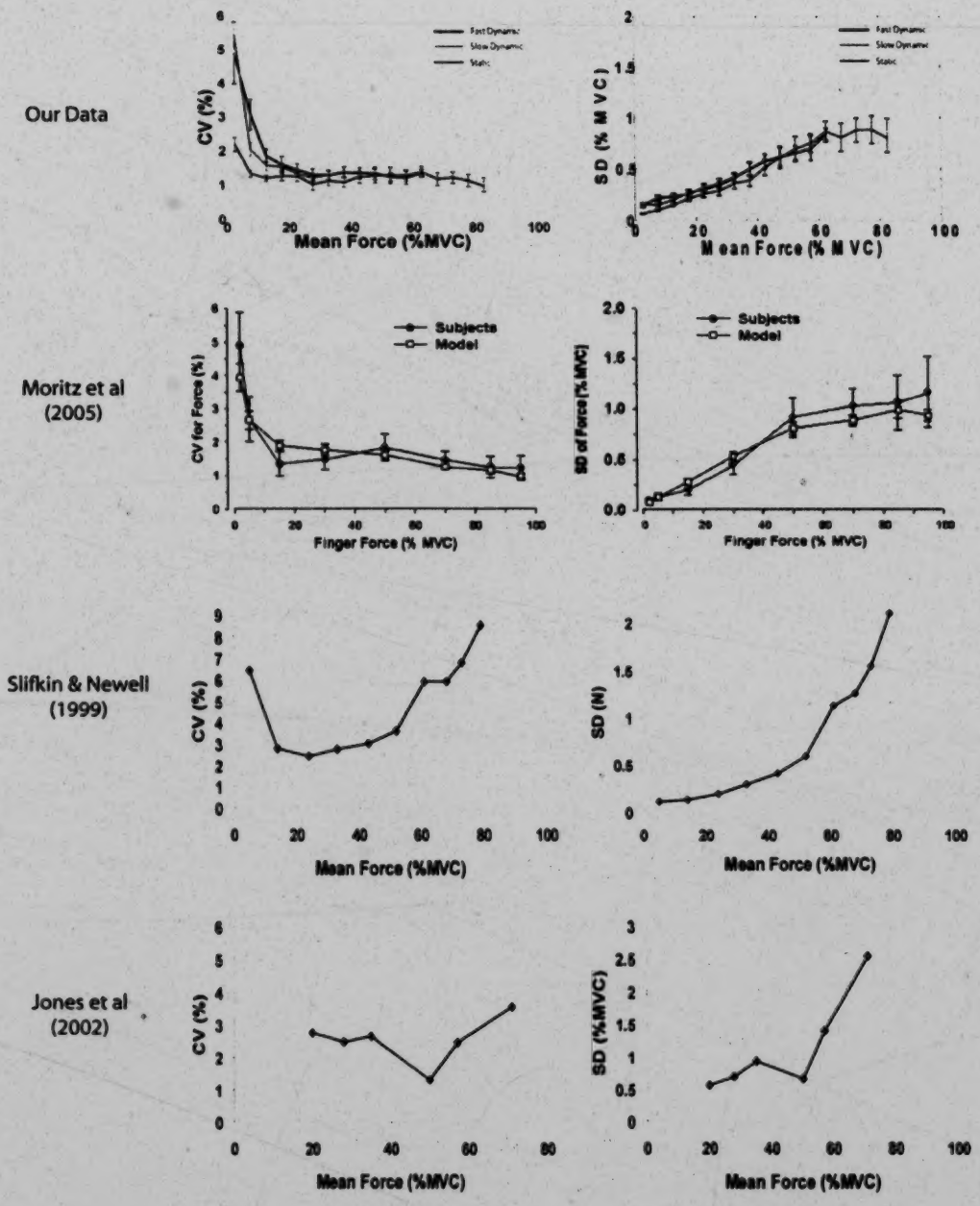

Fig 5.2: Comparison of CV and SD data from four studies. The Moritz figures are reproduced their paper (Moritz et al 2004). The Slifkin & Newell paper (1999) and the Jones paper (2002) only provided the graph for SD vs Mean, the CV curves for those two studies were estimated from the SD graph. Our data was most similar to the Moritz data.

There could be several explanations for the initial decrease in force CV. The firing rate of a motor neuron directly controls the force produced by the motor unit. There has been evidence to show that variability (CV) in the firing rate of motor units decreases as the level of force output increases, particularly at the low force range (Mortiz et al 2005, Laidlaw et al 2000). Thus, at low forces, the slow firing of the activated units could collectively contribute to the high force CV. Furthermore, as mentioned previously, deviation from a strict orderly recruitment can result in a higher force CV (Jones 2002). Since there are a greater number of small twitch motor units than large twitch units, the incremental increase in the synaptic drive required to recruit an additional motor unit is smaller at low forces than at higher forces. Consequently, there is a greater probability that two small twitch units with very close thresholds will interchange in the recruitment sequence, thus introducing some variation in the order of recruitment. Since at low forces, control of force output is primarily achieved through recruitment of motor units, any effects of recruitment variability will be more visible in this force range.

Thus, much of the available evidence seems to suggest that, for isometric contractions, the force output is characterized by a monotonically decreasing CV as the force level increases, over the entire force range. Moreover, much of the decrease occurs before 20%MVC. Hence, the CV can be considered to be effectively constant at higher forces, corresponding to a linear scaling between the SD and the mean force in that range. As such, the assumption of a linear SDN by Harris and Wolpert (1998) is at least true at force levels greater than 20%MVC. However, the non-linearity at the lower range of

force output could still have a significant impact on the outcomes of minimum variance control.

5.3 Effect of Non-linear SDN

Since we were unable to obtain the optimal motor commands and trajectories by applying the minimum variance control strategy under non-linear noise conditions, we were not able to directly determine if the non-linear noise would significantly alter the predictions of the control strategy. However, by applying non-linear noise to motor commands that were optimized for linear noise conditions, and determining the resulting wrist trajectories, we were able to show that the non-linearity in the SDN at low force levels does not significantly alter the trajectories and the magnitude of the end point variances. Thus, it is unlikely that the optimal command for such a non-linear noise would differ much from motor commands optimized for a linear noise, when applying minimum variance control. However, if the motor commands generated under the two noise conditions do differ significantly, then it would be likely that the nervous system would require different planning strategies for different directions of wrist movement, since in certain directions, non-linear noise produces a notable increase in the terminal variance than linear noise, even with the same motor command.

5.4 Limitations of the Wrist Model

The wrist model (Haruno 2005) used to determine the effects of a non-linear SDN, while informative and convenient, has a few limitations. First, the optimized motor commands

are stated in terms of arbitrary units, which do not correspond to any experimental measures of motor commands. If the motor commands could be normalized to an MVC, then it could be made comparable to experimental data. However, it is impossible to obtain, with precision, such an MVC for this model as there are no parameters in the model that can correspond to "maximum effort" in human or animal subjects. If a proper scaling factor or transfer function that can link the arbitrary unit of the model motor command to experimental measurements such as force or motor neuron firing rate can be obtained, then a more precise representation of the motor noise can be implemented in the model.

Second, with the non-linear, decreasing CV, the speed accuracy trade-off described by Fitt's law may no longer hold. With a higher CV at low forces and a lower CV at high forces, the linear wrist model should predict more accurate movements at higher speeds. However, the real musculoskeletal system is more complex than the simple linear model implemented here, which is likely missing certain features that may lead to movements which follow Fitt's law even in the presence of a non-linear SDN.

Finally, the wrist model is only a feed-forward model. It does not take into account the effects of sensory feedback. For instance, the delay in the visuomotor loop is approximately 150ms between the input of visual stimulus and observation of change in the motor output. The feedback information is used to make continuous adjustments to the movement and thus has a significant impact on the accuracy of the movement.

6 Conclusions & Future Work

The primary goals of this study were to determine: 1) if the level of force noise was changed by the type of contraction; 2) if the force noise scaled linearly with respect to the mean force; and 3) if a non-linear noise would affect the outcome of the minimum variance control strategy. It was found that different contraction types did indeed produce different levels of noise. It was also determined that, for static as well as dynamic contractions, the SDN did not scale linearly with the mean force, though the non-linearity was restricted to the low force range. For the last goal, we presented some evidence to suggest that a non-linear noise may not significantly affect the minimum variance. However, this evidence was inconclusive, and further work is needed to acquire better evidence. Some possible extensions from this work are discussed below.

The most immediate issue that can be addressed following the work done in this thesis is the calculation of the optimal motor commands under non-linear SDN conditions and determine whether the motor output (wrist activation patterns, arm trajectories, etc.) is significantly different from the simulated output under the previously assumed linear SDN conditions as well as real life behaviours.

Another point of potential improvement in this work is that the contractions performed in the experiments are all isometric. Movements in real life tend to be more isotonic. However, the difficulty in measuring the force generated in muscles during shortening or lengthening has restricted us to isometric contraction. If a technique to accurately

measure force during natural unconstrained movements were available, the noise during such movements can be characterized and applied to minimum variance control theory.

As a concluding remark, it must be noted that the minimum variance model is just one among a number of proposed models for motor planning. It has not been firmly established as the "best" model. While the minimum variance strategy seems quite suitable for goal directed tasks, other control strategies might be more appropriate under different conditions. For example, tasks involving extended periods of repetitive motions where accuracy is not of critical importance, such as running a marathon, the minimum energy strategy might be better suited. By testing the limits of current models, we will gain the knowledge to produce more accurate and robust models of motor control and hopefully gain a better understanding of the subject.

7 References

Berne RM, Levy MN, Koeppen BM, Stanton BA, Physiology. St. Louis: Mosby, 2003.

Burke, RE, DN Levine, M Salcman, and P Tsairis. Motor units in cat soleus muscle: physiological, histochemical, and morphological characteristics. J. Physiol(London). 238: 503-514, 1974.

Christensen E. Topography of terminal motor innervation in striated muscles from stillborn infants. Am J Phys Med. 38: 65-78, 1959

Clamann, PH. Statistical analysis of motor unit firing patterns in human skeletal muscle. Biophysics J. 9: 1233–1251, 1969.

Dean AF (1981) The variability of discharge of simple cells in cat striate cortex. Exp Brain Res 44:437-440

Dengler, R, Stein RB, et al. Axonal conduction velocity and force of single human motor units" Muscle Nerve 11:136, 1988.

Desmedt J, Godaux E. Ballistic contractions in fast or slow human muscles: discharge patterns of single motor units. J Physiol (London) 285:185-196, 1978.

Feinstein B, Lindegård B, Nyman E, and Wohlfart W. Morphologic studies of motor units in normal human muscles. Acta Anat. 23: 127-142, 1955.

Fitts PM. The information capacity of the human motor system in controlling the amplitude of movement. J Exp Psychol 47:381-391, 1954.

Flash T. and N Hogan . "The coordination of arm movements: an experimentally confirmed mathematical model." J. Neurosci. 5(7): 1688-1703, 1985.

Fugelvand AJ., Winter DA, and Patla A.E.. Models of recruitment and rate coding organization in motor-unit pools. J Neurophysiol 70: 2470–2488, 1993.

Harris, CM. and Wolpert DM. "Signal-dependent noise determines motor planning." Nature 394(6695): 780-784, 1998.

Hoffman, DS. and PL. Strick. "Step-Tracking Movements of the Wrist. IV. Muscle Activity Associated With Movements in Different Directions." J Neurophysiol 81(1): 319-333, 1999.

Jeannerod M. The neural and behavioral organization of goal-directed movements. Oxford: Clarendon Press, Oxford. 1988.

Jones, KE, A. F. d. C. Hamilton, et al.. "Sources of Signal-Dependent Noise During Isometric Force Production." J Neurophysiol **88**(3): 1533-1544, 2002.

Kitazawa, S. (2002). "Optimization of goal-directed movements in the cerebellum: a random walk hypothesis." Neuroscience Research 43(4): 289-294.

Lacquaniti, F., C. Terzuolo, et al.. "The law relating the kinematic and figural aspects of drawing movements." Acta Psychologica 54(1-3): 115-130, 1983.

Laidlaw DH, Bilodeau M, and Enoka RM. Steadiness is reduced and motor unit discharge is more variable in old adults. Muscle Nerve 23: 600-612, 2000.

Matthews, PBC. Relationship of firing intervals of human motor units to the trajectory of post-spike after-hyperpolarization and synaptic noise. J. Physiol. 492, 597–628,1996.

Martini FH. Fundamentals of Anatomy & Physiology. Bejamin Cummings. 2004.

McAdams, CJ and JHR. Maunsell. Effects of attention on orientation-tuning functions of single neurons in macaque cortical area V4. J. Neurosci. 19: 431–441, 1999.

Milner-Brown HS, Stein RB, et al.. "The orderly recruitment of human motor units during voluntary isometric contractions." J Physiol (Lond) 230:359, 1973.

Moritz CT, Barry BK, Pascoe MP, and Enoka RM. Discharge rate variability influences the variation in force fluctuations across the working range of a hand muscle. J Neurophysiol. First published December 22, 2004; 10.1152/jn.01122.2004.

Robinson, DA, Gordon JL, et al.. "A model of the smooth pursuit eye movement system." Biological Cybernetics 55(1): 43-57, 1986.

Salter, Chris. 2006. Pathology in Acute Polio. http://www.ott.zynet.co.uk/polio/lincolnshire/library/gawne/ppspandcm-s04.html (accessed July 10, 2006).

Schmidt, RA, Zelaznik H, Hawkins B, Frank JS, and Quinn JT. Motor-output variability: A theory for the accuracy of rapid motor acts. Psychol. Rev. 86: 415-451, 1979

Slifkin AB, and Newell KM. Noise, information transmission and force variability. J Exp Psychol Hum Percept Perform 25: 837-851, 1999.

Stein RB., Gosen ER, and Jones KE, "Neuronal variability: noise or part of the signal?," Nat. Rev. Neurosci. 6, 389, 2005).

Uno Y, Kawato M, Suzuki R. Formation and control of optimal trajectory in human arm movement. Biol Cybem 6 1:89-l01, 1989.

van der Helm FCT, and Rozendaal LA. Musculoskeletal systems with intrinsic and proprioceptive feedback. In: Biomechanics and Neural Control of Posture and Movement, edited by Winters JM, and Crago PE. New York: Springer-Verlag, 2000, p. 164-177.

Viviani, P. and Schneider, R.. A developmental study of the relationship between geometry and kinematics in drawing movements. J. Exp. Psychol. HPP, 17:198-218, 1991.

Wolpert, D. M. and Z. Ghahramani. "Computational principles of movement neuroscience." Nat Neurosci. 1991